Diplomarbeit

Influence of different drug shapes on biological effects in the lung

eingereicht von

Lisa Zellnitz

zur Erlangung des akademischen Grades

Doktorin der gesamten Heilkunde

(Dr.in med. univ.)

an der

Medizinischen Universität Graz

ausgeführt am

Zentrum für medizinische Forschung

unter der Anleitung von

Priv.-Doz.in Dr.in med. Dipl.Biochem. Eleonore Fröhlich

und

Assoz. Prof. Mag.pharm. Dr.rer.nat. Eva Roblegg

(Institut für Pharmazeutische Technologie & Biopharmazie,

Karl-Franzens-Universität Graz)

Graz, 21.02.2018

Statutory Declaration

I declare that I have authored this thesis independently, that I have not used other than the declared sources/resources, and that I have explicitly indicated all materials which have been quoted or paraphrased from the used sources.

Graz, 21.02.2018 *Signature: Lisa Zellnitz eh.*

Acknowledgments

First of all, I want to thank Priv.-Doz.in Dr.in med. Dipl.Biochem. Eleonore Fröhlich. She gave me the opportunity to write this diploma thesis under her supervision. Over the past months she always supported me with her expertise and answered all my questions patiently.

At this point I also want to sincerely thank Claudia Meindl, who sacrificed a lot of her time to show me how to work with cell cultures and supported me during all the cellular experiments.

A special thanks also goes to my second supervisor, Assoz. Prof. Mag.pharm. Dr.rer.nat. Eva Roblegg, from the Karl-Franzens-Universität Graz.

Furthermore, I want to thank Simone Pival-Marko from RCPE, who gave me the possibility to write my diploma thesis at RCPE in cooperation with the Medical University of Graz.

I also owe my gratitude to Ms Joana Pinto for her scientific support and help over all the time. Furthermore, I want to thank the RCPE lab team and the RCPE chroma team for helping me to carry out my experiments.

I cannot express the gratitude to my family enough. I want to thank my parents, Helga and Gert, for always believing in me and encouraging me throughout the last years. A special thanks also belongs to my grandparents, who not only supported my financially but also emotionally over the years of my studies. I also want to mention my brother, Stefan, who always listened to me when I had doubts or worries and never fails to cheer me up.
I am forever grateful to Dr.rer.nat Sarah Zellnitz, who is not only the best sister I could wish for, but also a great supervisor. Sarah supported the work on this thesis since the beginning and I want to thank her sincerely for her guidance and personal support over all the years.

Lastly, I want to thank all my friends who made the last six years of my studies so special and a time I will never forget.

Table of content

Abbreviations

AAT	α1-antitrypsin
ACOS	Asthma COPD overlap syndrome
ACT	Asthma control test
AECOPD	Acute exacerbation of COPD
AF	Alveolar fluid
ANS	Autonomic nervous system
API	Active pharamceutical ingredient
AT-I-cells	Type I alveolar cells
AT-II-cells	Type II alveolar cells
BHR	Bronchial hyperresponsiveness
BL	Basal lamina
cAMP	Cyclic adenosine monophosphate
CAT	COPD Assessment Test
CFTR	Cystic fibrosis transmembrane conductance regulator
CO_2	Carbon dioxide
COPD	Cronic obstructive pulmonary disease
CRP	C-reactive protein
DMEM	Dubeccos modified eagle medium
DPI	Dry powder inhaler
DPPC	1,2-Dipalmitoyl-sn-glycero-3-phosphocholine
DSC	Differential scanning calorimetry
DSV	Dead space volume
ECF-A	Eosinophil chemotactic factor of anaphylaxis
ED	Emitted dose
EDC	Endothelial cells
EDTA	Ethylenediaminetetraacetic acid
EPC	Pulmonary epithelial cells
FBS	Fetal bovine serum
FEF	Forced expiratory flow
FEV_1	Forced expiratory volume in one second
FPD	Fine particle dose
FPF	Fine particle fraction
FVC	Forced vital capacity
GINA	Global Initiative for Asthma

GOLD	Global Initiative for Obstructive Lung Diseases
HPLC	High performance liquid chromatography
ICS	Inhalable corticosteroids
Ig-E	Immunglobuline E
JM SS	Jet-milled salbutamol sulphate
kPa	Kilopascal
KRB	Krebs-Ringer-Buffer
LABA	Long-acting beta-agonist
LAMA	Long-acting muscarinic antagonist
LH100	Lactohale 100
LVRS	Lung volume reduction surgery
MDI	Metered dose inhaler
MEF	Mid expiratory flow
MEM	Minimum essential medium
MMAD	Mass median aerodynamic diameter
mmHg	Millimetres of mercury
mMRC	Modified British Medical Research Council
MPS	Mononuclear phagocyte system
NGI	Next Generation Impactor
NSAIDs	Non-steroidal anti-inflammatory drugs
$PaCO_2$	Partial pressure of carbon dioxide
PaO_2	Partial pressure of oxygen
PDE	Phosphodiesterase
PDF-4	Phosphodiesterase-4
PEF	Peak expiratory flow rate
pH	Potential of hydrogen
pMDI	Pressurized metered dose inhaler
PSD	Particle size distribution
RBC	Red blood cells
RSD	Relative standard deviation
SABA	Short-acting beta-agonist
SAMA	Short-acting muscarinic antagonist
SD	Standard deviation

SEM	Scanning electron microscope
SLF	Simulated lung fluid
SP	Surfactant protein
SS	Salbutamol sulphate
SWAXS	Small and wide angle x-ray scattering
TEER	Transepithelial electrical resistance
VC	Vital capacity
WAXS	Wide angle x-ray scattering

List of figures

List of tables

Zusammenfassung

Damit Wirkstoffe die Lunge erreichen, müssen sie eine Größe zwischen 1 und 5 µm aufweisen. Um Wirkstoffe dieser Größe herzustellen, werden unterschiedliche Verfahren angewendet, wie Mahlen oder Sprühtrocknen. Als Modellwirkstoff für diese Arbeit wurde Salbutamol Sulfat (SS) verwendet. Ein Wirkstoff, der zur Gruppe der ß2-Sympathomimetika gezählt wird und in der Therapie von chronisch obstruktiven Lungenerkrankungen (COPD) und Asthma bronchiale eingesetzt wird. In bisherigen Studien konnte gezeigt werden, dass Luftstrahlmahlung von SS nadelförmige, kristalline Partikel erzeugt. Durch Sprühtrocknung hingegen werden runde, amorphe Partikel hergestellt. Ob, und vor allem wie, sich die Form der Partikel auf die Wirkstoffaufnahme in Lungenzellen auswirkt, ist von großer wissenschaftlicher und medizinischer Bedeutung und zentraler Bestandteil dieser Arbeit. Um die Wirkstoffaufnahme der unterschiedlich geformten Partikel in den Lungenzellen zu testen, wurden sowohl Permeabilitätsstudien, als auch zelluläre Aufnahme-Experimente durchgeführt, wobei unterschiedliche Zellarten verwendet wurden. Für die Permeabilitätsstudien wurden A549 Zellen, welche ein etabliertes Model für Typ-I-Alveolarzellen darstellen, sowie Calu-3 Zellen verwendet. Um die zelluläre Aufnahme zu testen wurden A549 und DMBM-2 Zellen, welche alveolare Makrophagen repräsentieren, verwendet. Neben den Zellversuchen wurden Formulierungen der unterschiedlichen Partikel mit einem Modellträger (Lactohale 100) hergestellt und die *in-vitro* Lungengängigkeit mittels eines Impaktors ermittelt. Zusätzlich wurden der Zerfall und die Löslichkeit der unterschiedlichen Wirkstoffformulierungen mittels Dissolution getestet.

Es konnte gezeigt werden, dass gemahlene, nadelförmige Partikel eine höhere Lungengängigkeit als sprühgetrocknete Partikel aufweisen. Sprühgetrocknete Partikel zeigten jedoch einen höheren Permeabilitätskoeffizienten (P_{app}) und eine schnellere, höhere Aufnahme durch Makrophagen. Beide Partikelformen zeigten ähnliche Ergebnisse hinsichtlich ihrer Löslichkeit und nach etwa zwei Minuten waren die Partikel vollständig gelöst. Die rasche Löslichkeit der Partikel schließt eine Aufnahme der Partikel via Phagocytose weitgehend aus, sodass andere Aufnahmemechanismen in Kraft treten müssen. Für zukünftige Studien soll ein Wirkstoff mit schlechterer Löslichkeit gewählt werden, um den Einfluss der Wirkstoffform genauer untersuchen zu können.

Abstract

For administering active pharmaceutical ingredients (APIs) to the lung, a particle size of 1-5 µm is needed. The most common technique to generate small, inhalable sized particles is milling of the API, but spray drying has shown to be a suitable alternative. Both techniques lead to inhalable sized particles but the shape of the particles and other properties, e.g. solid-state, can vary. The model drug chosen for this study is salbutamol sulphate (SS). It is a beta-2 agonist and a frequently used drug in the treatment of bronchial asthma and COPD (chronic obstructive pulmonary disease). Previous studies showed that spray drying of SS creates spherically shaped, amorphous particles, whereas milling normally keeps the needle-like shape of the drug crystals. The aim of this work was to identify whether the particle shape has an influence on the biological effects of the inhalable particles in the lung. Permeability experiments and cellular uptake experiments were performed, using distinct cell lines: Calu-3 cells were used for permeability testing and DMBM-2 cells, which represent alveolar macrophages, were used for cellular uptake experiments. A549 cells, which represent a well-established model for type-I-alveolar cells, were used for both experimental set ups. Inhalable formulations were prepared with jet-milled and spray dried SS particles and Lactohale 100 (LH100) as a model carrier. The different formulations were used for determining the dissolution behaviour of the particles, as well as the in-vitro respirable fraction, which was tested with a next generation impactor (NGI). Jet-milled particles resulted in higher respirable fractions, compared to spray dried particles. This has already been shown in previous studies. Regarding the cellular experiments, lower apparent permeability coefficient values (P_{app}-values) and lower uptake in macrophages could be shown for jet-milled particles. Spray dried, spherically shaped particles, showed higher epithelial permeability and higher uptake by macrophages. However, both formulations showed similar dissolution behaviour and dissolution was almost complete after 2 minutes. This fact makes a prominent influence of phagocytosis rather unlikely and leads to the suggestion that distinct uptake-mechanisms must occur. It is possible that, after partial dissolution, the crystalline particles were in the range for preferential active uptake by epithelial cells. For future experiments, an API with lower solubility will be chosen in order to get detailed insight on the impact of particle shape.

1 Introduction

1.1 Respiratory system

The main function of the respiratory system is the gas exchange between air and blood. During this process, oxygen is added to the blood and carbon dioxide, which arises during metabolic processes in our body, is emitted. This vitally important function takes place in the last part of the respiratory system, the so called acini, and the capillary system which surrounds the acini.

Topographically the human respiratory system can be separated into upper and lower airways. Whereas the upper airways, which include the nasal cavity, the pharynx and the larynx, are the main components for taking up air and oxygen, the lower airways are responsible for transporting the air into the acini and executing the gas exchange. In the following section, the lower airways and the bronchial system will be described in more detail (1).

1.1.1 Lower airways

The lower airways in general include all airways downwards from the trachea, including the trachea itself. The trachea also marks the origin of the bronchial-system. It is a highly branched and complex system, resembling a tree and therefore also called bronchial tree. It consists of 23 generations, initiating at the trachea (level 0) and ending at the acini (level 23). However, the number of generations may vary and usually ranges from 18-30 (2). Each airway is dichotomously divided into two smaller daughter airways. This model was published by Weibel in 1963 and is called his “A”-model. It is one of the simplest models of the human lung and therefore widely used. Figure 1 gives a schematic overview of the respiratory system (3).

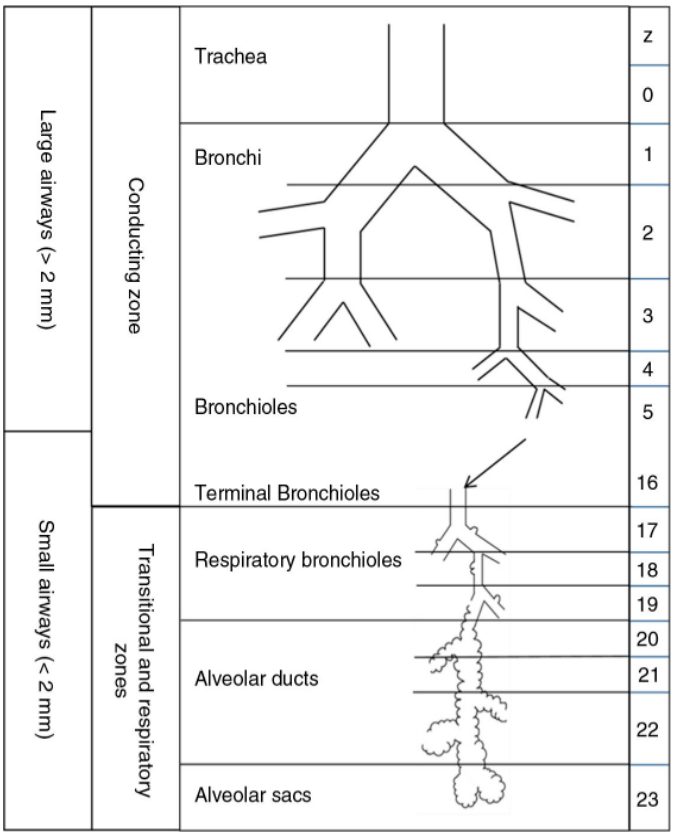

Figure 1: Anatomy of the respiratory system (4)

Weibel divided all 23 airway generations into upper and lower generations. The main function of the upper generations, which include all airways from level 0 to approximately level 16, is the air conduction. In these sections the inhaled air is warmed, humidified and roughly cleaned by the epithelial layer of the inner walls, which will be described in more detail in section 1.1.3.

No gas exchange takes place in this part of the bronchial tree and the transported volume is called dead space volume (DSV). All generations that follow afterwards are summarized as respiratory parts (2,3).

1.1.1.1 Anatomy of the bronchial tree

The initial component of the bronchial tree is the trachea. It is a 10-12 cm long elastic pipe with a diameter of 1.5-2 cm. The trachea is stabilised through cartilage rings, open at the posterior side, so that it will not collapse during inspiration. At the height of the fourth thoracic vertebral body the trachea divides itself into the two main bronchi.

The right main bronchus is about 1.5-2 cm long and significantly shorter than the left main bronchus, which measures approximately 4 cm.

The diameters of the main bronchi range from 12-14 mm. The two main bronchi then split up into the lobar bronchi. In the right lung there are three lobar bronchi: Bronchus lobaris superior, medius and inferior. Contrary to this, the left lung possesses only a bronchus lobaris superior and a bronchus lobaris inferior. Based on the anatomy of the lobar bronchi, the right and the left lung can be divided into different lobes (5 in total). The lobar bronchi, which have an approximate diameter of 8 mm, divide into the segmental bronchi, which separate the lung into even smaller compartments, called segments. Each lung consists of ten segments.

At the end of multiple divisions (approximately 6-12 steps) the segmental bronchi lead into the terminal bronchioles. With an approximate diameter of <0.4 mm, the terminal bronchioles mark the end of the air conducting parts of the respiratory system and typically start at generation 14-16. All generations that follow after the terminal bronchioles contribute to the gas exchange and can be summarized under the term “acinus”.

The respiratory bronchioles rise from the terminal bronchioles. They have an approximate diameter of 0.4 mm and merge into the alveolar ducts.
These are small ducts that, after about 5 divisions, lead into the final generation of the respiratory system, the alveolar sacs. Whereas the respiratory bronchioles contain only a few pulmonary alveoli in their wall, the alveolar ducts are composed of pulmonary alveoli being tightly stringed together (5,6). This can also be seen in Figure 1: Anatomy of the respiratory system.

Overall it can be observed that the diameters and the length of the bronchial airways become reduced with each generation but the number of divisions increases and therefore also the number of airways. As a result, the total cross-sectional area of all airways increases with each division. These conditions influence the velocity of the inhaled air, which is highest in the upper airway generations and lowers with each division of the bronchial tree (4,7).

1.1.2 Pulmonary Alveoli

Pulmonary alveoli are air-filled compartments with an approximate diameter of 250 µm. The human lung possesses about 300-400 million pulmonary alveoli which are tightly stringed together, separated only through thin intra-alveolar septa. These septa work as frames for the dense capillary system.

Based on this specific composition, the capillary system and the alveoli are in direct contact and the gas exchange can take place between these two components.

The inner surface of the pulmonary alveoli is lined with the alveolar epithelium, which consists of two main cell-types: Type I alveolar cells (AT-I-cells) and type II alveolar cells (AT-II-cells), often also called alveolar pneumocytes. All cells of the alveolar epithelium are connected through tight junctions.

Type I alveolar cells: These cells make up approximately 95% of the surface of the pulmonary alveoli. They contain few cell organelles and show poor metabolic activity. With their large and thin cell bodies, type I alveolar cells are in close contact with endothelial cells of the capillary system and are part of the blood-air barrier, which as a whole consists of the following three components:
The capillary endothelia, a shared basal lamina and the tails of AT-I-cells. The thickness of the blood-air barrier in the human lung has an average value of 0.6 µm. This value represents the distance between the air inside the pulmonary alveoli and the blood inside the capillary system and therefore has to be overcome during gas exchange. This is illustrated in Figure 2. The figure shows the endothelial cells of the capillary system (EDC), the pulmonary epithelial cells (EPC) and the basal lamina (BL). Furthermore, red blood cells (RBC) and the alveolar fluid (AF) are illustrated.

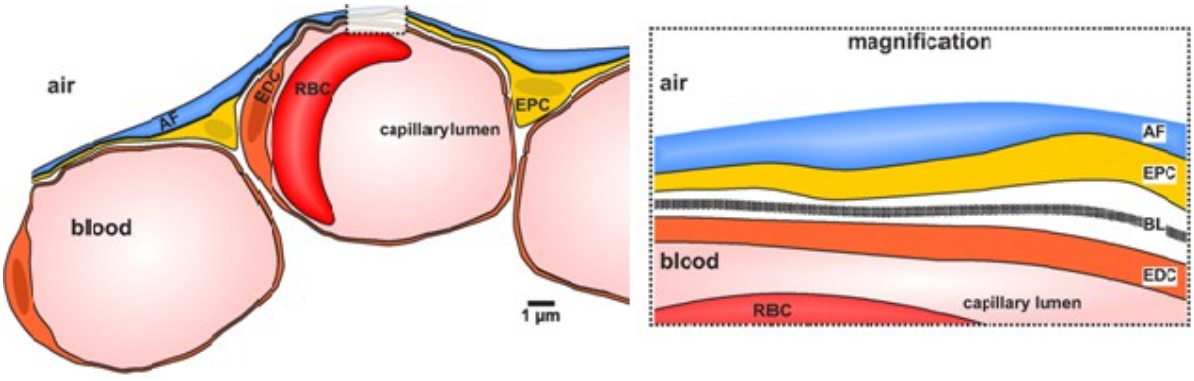

Figure 2: Components of the blood-air-barrier (8)

Type II alveolar cells: Type II alveolar cells are cubic cells, resting in small niches and therefore covering only 5-7% of the alveolar surface. The main function of this cell-type is the production of surfactant, which will be described in more detail

below. Furthermore, type II cells act as progenitor cells for both type I and type II cells, meaning that they can replace damaged cells (5,9,10).

Surfactant: The inner surface of the pulmonary alveoli is not in direct contact with the air inside the pulmonary alveoli since it is covered with a fluid, watery film. Because of the high surface tension at this gaseous-aqueous interphase, the pulmonary alveoli would collapse during expiration. Surfactant decreases the surface tension and consequently is an essential factor for maintaining the structure of the pulmonary alveoli during gas exchange. It consists of 90% phospholipids and 10% surfactant proteins.

Phospholipids are amphiphilic compounds, which means that they possess both lipophilic (fat-loving) and hydrophilic (water-loving) properties. They can layer themselves onto the watery film of the alveolar epithelium and prevent the pulmonary alveoli from collapsing. The main phospholipids are Phosphatidylcholine and Phosphatidylglycerol. Regarding surfactant proteins (SP), four different types occur: SP-A, SP-B, SP-C and SP-D. SP-A and SP-D are hydrophilic proteins, SP-B and SP-C show hydrophobic character. The latter contribute in structural organization of surfactant at the gaseous-aqueous interphase, whereas the hydrophilic components have immunological functions. For example, SP-D plays an important role in activating alveolar macrophages. Additionally, SP-A and SP-D proteins have an impact on the secretion of surfactant and surfactant reuptake in AT-II-cells.

As already mentioned above, surfactant is produced by type II alveolar cells. These cells feature lamellar bodies inside their cell bodies, so they can store phospholipids and surfactant. The cells release surfactant through exocytose. The synthesis and the secretion of surfactant are controlled by complex metabolic and genetic mechanisms. Furthermore, synthesis of surfactant phospholipids, especially of phosphatidylcholine, is also regulated hormonally. For example, thyroid hormones, glucocorticoids, prolactin and estrogen increase the synthesis of surfactant (5,10).

Alveolar macrophages: These cells are phagocytes, located in the alveolar epithelia. They are important for cleaning the terminal parts of the bronchial tree, which do not possess ciliated epithelia. Alveolar macrophages do not only take up air-borne particles via phagocytosis, but also dead cells and pathogenic germs.

Thereafter they migrate towards the ciliated epithelia of the air-conducting airways, where they are segregated together with the mucus. In some cases they can also be deposited in the connective tissue of the lung and form so called anthracotic pigments. Furthermore they can enter the lymphatic system.
The alveolar macrophages are part of the human mononuclear phagocyte system (MPS), which is a summarizing term for all macrophages of the human body (5,9).

1.1.3 Epithelia of the respiratory system

The epithelium, which covers the air-conducting parts of the human lung, has a specific structure and appears only in the respiratory system, for which reason it is also called respiratory epithelium. It is a multiple-rowed, ciliated epithelium with interspersed goblet cells.

Ciliated cells feature kinocilia and microvilli on their apical surface. Due to that they can transport mucus and therefore contribute essentially to the clearance of the lung. The ciliated cells are located on basal cells and a basal lamina. These basal cells additionally work as progenitor cells and can replace dead cells through proliferation. Pulmonary goblet cells represent another main structure of the respiratory epithelium. They produce mucus, which then forms a mucus layer on top of the epithelia of the respiratory airways. This mucus layer collects polluted particles from the inhaled air. Through tiny movements of the kinocilia and the microvilli, the mucus is transported towards the pharynx, where it is generally swallowed. Particles >10 µm usually are collected in the upper airways, whereas smaller particles (5-8 µm) are captured in the trachea or the bronchial system. Particles smaller than 5 µm can make their way into the alveolar system. However, the smaller the bronchial system gets, the less the airways feature ciliated cells and pulmonary goblet cells in their epithelium. In the final sections of the respiratory system, these structures, and as a result also the mucus layer, are entirely missing. According to this, polluted particles reaching these sections can only be eliminated by alveolar macrophages, as described in Pulmonary Alveoli.
Instead of ciliated cells, the small respiratory airways (meaning all compartments downwards from the terminal bronchioles with a diameter of less than 2 mm) feature more club cells (formerly “clara cells”) in their walls. These cells also secrete the surfactant proteins SP-A and SP-D, as well as the club cell 10 kDa protein. All three of these factors have anti-inflammatory effects.

In addition there are two more cell-types in the epithelium of the respiratory airways: Neuroendocrine cells and brush cells. Brush cells are small cells with microvilli on their surface and work as chemo receptors. The neuroendocrine cells are part of the diffuse neuroendocrine system of the human body. They can release serotonin and different peptide hormones. Furthermore these cells are the point of origin for the development of the highly malignant small cell lung cancer, which represents about 25% of all cancer-types in the lung (5,9,11).

1.2 Obstructive lung diseases

Obstructive lung diseases are characterized by shortness of breath and narrowing of airways. These diseases include COPD, bronchial asthma, bronchiectasis and cystic fibrosis.

Bronchiectasis is characterized by the presence of structurally abnormal, sack-like bronchi. These abnormalities are the result of a destruction of muscles and connective tissue in the bronchi, caused by persistent airway infection and recurrent exacerbations. The disease occurs with a frequency of 27 (m) - 35 (f) cases/100.000 patient-years (12,13).

Cystic fibrosis is an autosomal recessive inherited, genetic disorder, which shows a prevalence of 0.73/10.000 patient-years in Europe (14). The symptoms are caused by a mutation of the CFTR (cystic fibrosis transmembrane conductance regulator) gene on chromosome 7. This mutation leads to a dysfunction of the chloride channels in exocrine glands. As a result, these glands segregate extremely viscous mucus, which causes an obstruction of the glands and the excretory duct. Airways, pancreas, the male genital system, intestine, liver, bone, and kidney can be involved (12,15). Compared to the prevalence of asthma (6%) and COPD (4%) in Europe, the former two are rare diseases (16).

1.2.1 Bronchial Asthma

Bronchial asthma is a chronic respiratory disease, caused by a chronic inflammation of the respiratory system. It is characterised by bronchial hyperresponsiveness (BHR) and a respiratory obstruction, which is partially reversible.

Due to aetiology there are two main groups of bronchial asthma: Allergic bronchial asthma and non-allergic bronchial asthma. In both cases the main symptom is paroxysmal dyspnoea (12,17).

1.2.1.1 Epidemiology

Bronchial asthma is a widely spread disease. About 5% of adults and 10% of children suffer from bronchial asthma, which occurs more frequently in men (m:w=2:1). Furthermore, differences of prevalence can be observed. In 2012 the global prevalence of clinically diagnosed asthma was 4.5%, whereas the prevalence of bronchial asthma in Austria was approximately 7.6% (18).

1.2.1.2 Aetiology and pathogenesis

As mentioned above, bronchial asthma can be divided into two main subcategories due to aetiology. Furthermore, also mixed types can occur.

Allergic bronchial asthma (extrinsic asthma)

This type of asthma usually occurs for the first time at infancy and is often associated with other atopic diseases, such as conjunctivitis, rhinitis or dermatitis (19). Animal hair, plants, pollen, mould fungus and other substances, such as chemicals or house dust, can provoke an Ig-E mediated type-I allergic reaction. During this reaction, mast cells discharge different inflammatory mediators, like histamine, eosinophil chemotactic factor of anaphylaxis (ECF-A), leukotriene and bradykinin. The secretion of these factors causes an inflammatory reaction in the respiratory airways and within minutes leads to a bronchial constriction (allergic early phase response). Due to the chronic airway inflammation, structural changes of the bronchial walls take place (airway remodelling). Studies showed that administered steroids in asthmatic patients do not only reduce the inflammation of respiratory airways, but also show beneficial effects on airway remodelling. Regarding these results, chronic airway inflammation is believed to be the main factor for airway remodelling. The remodelling processes include a hypertrophy and hyperplasia of the smooth muscle cells in the bronchial walls, bronchospasm, mucosal edema development and a hyperplasia of the goblet cells. Furthermore, an increase of mucus production and higher viscosity of the mucus (dyscrinism) occur. All of these modifications cause an endobronchial obstruction which results in a reduction of the airflow in the lung (12,19,20).

Non-allergic bronchial asthma (intrinsic asthma)

Most frequently non-allergic bronchial asthma is provoked by respiratory infects. Furthermore it can be triggered by chemical or toxic substances, physical effort (especially among teenagers) or analgesics. All of these factors induce inflammatory processes and ultimately lead to an endobronchial obstruction, as described above.

The analgesic induced bronchial asthma is a special type of asthma which occurs mainly in adults. It is also called analgesic asthma syndrome and usually is caused by NSAIDs (non-steroidal anti-inflammatory drugs) or acetylsalicylic acid. These substances provoke a pseudoallergic reaction, which also leads to a discharge of inflammatory mediators from mast cells. Contrary to Ig-E mediated type-I-allergic reactions, pseudoallergic reactions have no sensitizing phase and appear at the first contact with the triggering substance (12,17,19).

The more often the respiratory system is exposed to the triggers, the more sensitive it gets and after some time BHR can be observed. This means, that a bronchial constriction can also be caused by unspecific triggers, for example cold and wet air. The constriction is caused by a contraction of the smooth muscles and an increased mucus production. The pathogenesis of the BHR, often also referred to as bronchial hyper reactivity, is not completely understood. It is believed tough, that the parasympathetic component of the autonomic nervous system (ANS) represents a main factor. An altered activity of the vagus nerve causes the muscle contraction and therefore leads to airflow limitation. BHR occurs in all types of bronchial asthma and can be identified with metacholine provocation tests, described in section 1.2.1.4. (21,22).

1.2.1.3 Clinical symptoms

The main symptoms of bronchial asthma are the following: Paroxysmal dyspnoea, which is the leading symptom, cough, expiratory wheezing and thoracic tightness. The symptoms often appear during the night and in between asthmatic seizures patients often have symptom-free intervals. Furthermore, patients who suffer from allergic bronchial asthma, frequently show symptoms only during specific seasons (seasonal bronchial asthma), when they are exposed to the triggering substance.

The status asthmaticus is a dreaded complication of bronchial asthma. It is a severe asthmatic exacerbation, which develops rapidly. The symptoms are not treatable with short-acting bronchodilators, although these drugs normally are used as first-line therapy during an acute asthma seizure. The status asthmaticus is a medical emergency and therefore should be treated at an intensive care unit. The progressive bronchial constriction causes a ventilation/perfusion imbalance, hyperinflation and after some time respiratory muscle failure may arise because of increased breathing work. As a result, respiratory insufficiency occurs. The treatment of a status asthmaticus includes the administration of short-acting beta agonists via nebulisation, oxygen therapy and systemic corticosteroids. Patients not responding to the inhaled therapy, have to be intubated (23).

1.2.1.4 Diagnosis

In many cases the diagnosis can be made based on the specific symptoms during an asthma seizure. However, the leading symptom of paroxysmal dyspnoea can be absent and some patients primarily suffer from severe cough (so called *"cough variant asthma"*), which makes the diagnosis more difficult.

During lung auscultation, rales sounds, as well as expiratory rhonchi and humming, can be heard. Furthermore, the expiratory phase is elongated and the respiratory frequency is elevated. In some cases the bronchial constriction leads to pulmonary emphysema and therefore few or no breathing sounds can be noticed during auscultation (silent lung).

Another important step for diagnosing bronchial asthma is doing a blood examination, which delivers advantageous information. For example, inflammatory parameters will increase when bronchial asthma is caused by a respiratory infection. On the contrary, allergic bronchial asthma is likely when eosinophilic granulocytes are high in number and the total amount of Ig-E is raised.
Blood gas analysis gives information about the severity of the respiratory insufficiency, which is especially important during a status asthmaticus.

As for apparitive diagnostic, several tools can be helpful, but by far the most important ones are pulmonary function tests, carried out with different systems, such as spirometry or bodyplethismography. Spirometry is the timed measurement of dynamic lung volumes. Various parameters can be measured, which then

provide information about the pulmonary function. Important parameters, relating to the diagnosis of bronchial asthma, are the FEV_1, the PEF and the $FEF_{50.}$ All three of these values are reduced in patients suffering from bronchial asthma and will be described in more detail below (12,19,24).

FEV_1 (forced expiratory volume in one second): For determining the FEV_1-value, patients have to inhale as long and deep as possible and then exhale the air forcefully within one second. If the FEV_1 is reduced, it is a sign for a bronchial obstruction. The standard values of the FEV_1 should be higher than 75% of the vital capacity, but they depend on the age of the patient as well as on the performance of the patient during the test. The VC is the maximum amount of air that can be exhaled after a deep inhalation. The measured FEV_1 value is often related to the Forced Vital Capacity (FVC), which is defined as total expiratory volume during a maximally forced expiration manoeuvre. The FEV_1/FCV ratio is a helpful parameter to distinguish lung diseases with airway obstruction (obstructive lung diseases) from lung diseases with reduced lung volume (restrictive lung diseases). If the calculated value is less than 0.7, an obstructive pulmonary disease is likely. For restrictive pulmonary diseases the FEV_1/FCV value is normal (19,25).

PEF (peak expiratory flow rate): The peak expiratory flow represents a person's maximum speed of expiration during forced expiration. It is not only a meaningful value for diagnosing bronchial asthma, but it is also a good parameter for patients to follow up the progression of their disease. With a peak-flow-meter patients can measure the PEF autonomously at home. These measurements should be done in the morning, where the measured values are the lowest, and at night, where the PEF normally is the highest. Fluctuations of more than 20% indicate an inadequately treated bronchial asthma. The PEF is measured in l/sec or l/min. The values are dependent on age, sex and body height and can be looked up in specific tables. A PEF < 100 l/min during an asthmatic seizure indicates a severe development (12,19,25).

MEF (mid expiratory flow): MEF_{25}, MEF_{50} and MEF_{75} describe the maximal expiratory flow at 25%, 50% and 75% of the FCV. For example, MEF_{75} is the value, where 75% of the FCV are still in the lung and remain to be exhaled. These

values are used for estimating at which sector of the bronchial system the obstruction appears. For example, an obstruction of the smallest airways in the lung will lead to a diminution of MEF_{25}. For bronchial asthma in most cases MEF_{50} is reduced. The maximal expiratory flow values are measured in l/sec. However, in some studies and books only FEF_{25}, FEF_{50} and FEF_{75} (forced expiratory flow) are described. These values indicate the expiratory flow rates, when a specific percentage (x%) of the FCV has already been exhaled (FEF_x). The two values correlate the following way: The MEF_{25}, for example, is the expiratory flow rate where 75% of the FCV have already been exhaled and therefore mirrors the FEF_{75} (24,26).

When performing spirometer tests, the volume of the inhaled and exhaled air will be recorded over the time. The software of the spirometer will then deliver a so called spirogram, which illustrates a flow-volume loop and a volume-time curve. As for the flow-volume loop, the y-axis depicts the rate of airflow and the x-axis the volume of inhaled or exhaled air, shown in Figure 3. The flow-volume loop graphically displays the values mentioned above.

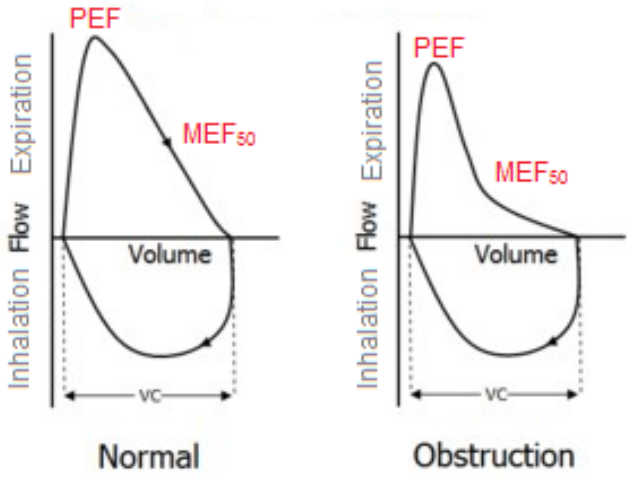

Figure 3: Flow volume loop. Modified from (27).

In some cases bronchodilator reversibility testing is performed to differentiate between reversible and non-reversible bronchial obstructions and to confirm the diagnosis of bronchial asthma. Standard spirometry tests are done and afterwards the patients have to inhale a bronchodilating drug, in most cases ß2-sympatomimetikas, such as salbutamol sulphate. After ten minutes, the spirometry test is repeated. If the FEV_1 increases more than 15% or 200 ml, compared to the

pre-bronchodilator value, the bronchodilator reversibility test is positive and the diagnosis of bronchial asthma is very likely (12,19).

When standard lung function tests do not show explicit signs of an obstructive lung disease, but symptoms suggest bronchial asthma, a so called challenge test can be done. With this method, the bronchial system is tested for hyperresponsiveness, which represents a characteristic mechanism in the pathogenesis of bronchial asthma. Drugs, which show bronchospasmolytic effects, are administered and the changes of FEV_1 are observed. The most frequently used drug is metacholine, why this test is also known as metacholine challenge test or metacholine provocation test. If the FEV_1 decreases more than 20% from the primarily tested value, bronchial asthma is most likely to occur. Also, a gain of the pulmonary resistance of more than 100% is characteristic for bronchial asthma. The pulmonary resistance is measured with bodyplethismography (19).

Summarized up, bronchial asthma can be diagnosed with certainty if the following criteria appear: a characteristic anamnesis and asthma specific clinical symptoms, reduced lung-function values and a positive bronchodilator reversibility test.

1.2.1.5 Therapy

The main goal of the asthma therapy is to control and to stabilise the course of the disease, so that asthmatic seizures are reduced and patients are symptom-free during night and day. The therapy of bronchial asthma does not only include pharmacological treatment, but also causal therapy strategies, which have a high significance. For example, people suffering from allergic bronchial asthma should avoid contact with the triggering substance and a hyposensitization therapy should be considered. In patients, who show non-allergic bronchial asthma, respiratory infects should be treated immediately to avoid exacerbations.

Every year, GINA (Global Initiative for Asthma) releases new guidelines, not only giving information about the pharmacological asthma treatment, but also about the diagnosis and the classification of bronchial asthma.

In general, the medical therapy of bronchial asthma can be subdivided into two main groups, called “controllers” and “relievers”. Controllers are drugs that, as the name suggests, are taken constantly to control the disease and show anti-

inflammatory effects. In contrast, relievers are bronchodilating drugs, taken during an acute seizure and providing rapid amelioration.

The medical treatment of bronchial asthma is known as a “step-up/step-down treatment”. This means that after 3 months, in which the disease has been under control, the medication can be reduced. However, it also means that, if the patient is suffering from symptoms and the disease is not well medicated, the therapy has to be adapted. This could require either a raise of the drug dosage, or the inclusion of other drugs to the treatment plan (12).

To evaluate if the disease is under control, different questionnaires for asthma patients have been established, but the asthma control test (ACT) is the one most frequently used. This test refers to a period of four weeks and includes five questions about asthmatic symptoms during day and night, the demand of reliever medication and how the disease has affected the daily life of the patients. For each question, five possible answers can be chosen. In the end, a maximum of 25 points can be reached, which would mean, that the disease is completely under control (28).

Concerning the pharmacological treatment, GINA released a 5-step-scheme, which should be used as a guideline in asthma therapy (Table 1).

Purpose	Step 1	Step 2	Step 3	Step 4	Step 5
Controller					"Add-on" therapy
			LABA	LABA	LABA
		Low dose inhalable corticosteroids	Low dose inhalable corticosteroids	Medium/high dose inhalable corticosteroids	Medium/high dose inhalable corticosteroids
Reliever	SABA	SABA	SABA	SABA	SABA

Table 1: Guideline for the pharmacological treatment of bronchial asthma (29)

In step 1, patients use relievers only in case of asthmatic seizures and do not take permanent medication. The relievers mainly are represented through short-acting beta agonists (SABAs), which will be described in more detail in section 1.4. If the patient has to use the relievers more than four times a week, a step up in the treatment plan should be considered.

In step 2, low dose inhalable glucocorticoids (ICS), like beclometasone and budesonide, are added to the medical treatment. These substances have an anti-inflammatory effect and reduce the chronic bronchial inflammation, therefore leading to an improvement of the symptoms. If symptoms cannot be controlled with these medications, long-acting beta agonists (LABAs), such as formoterol or salmeterol, are added to the treatment plan in step 3. If no improvement can be achieved, step 4 requests a dose increase of the inhalable glucocorticoids. Step 5, which is the final step of the scheme, foresees the inclusion of “add-on” therapies, like omalizumab, mepolizumab or tiotropium bromide. Omalizmuab is an anti-Ig-E antibody and is only administered to patients older than 12 years who suffer from allergic bronchial asthma. Mepolizumab, which is a mononuclear antibody against IL-5, and tiotropium bromide, which is a long-acting anticholinergic bronchodilator, should also only be administered if all previous treatments have failed and the patients are older than 12 years. In step 2, 3 and 4, leukotriene receptor antagonists, like montelucast, and theophylline can be used additionally (12,29,30).

For optimising the therapy of bronchial asthma, the knowledge of patients about their disease and their active cooperation play an essential role. As mentioned before, patients are asked to measure their PEF-values twice a day and record the values. Due to their PEF-values, patients can be categorized into three differently coloured groups: green, yellow and red.
The classification is based on the highest PEF-value a patient personally has ever achieved. Patients who are symptom-free and whose PEF-values range from 80-100% of their personal maximum value, belong to the green group.
If the peak flow represents 50-80% of the maximum value, patients are categorized as “yellow”. For amelioration of the symptoms, SABAs should be taken and an adaption of the asthma therapy should be carried out as soon as possible. If a person has PEF-values lower than 50% of its best value, he will be added to the red group. This means that the patient should take his emergency medication and consult a doctor immediately (12).

1.2.2 Chronic obstructive pulmonary disease

Chronic obstructive pulmonary disease (COPD) is a progressive disease, which causes irreversible airway obstruction. COPD is mostly caused by tobacco smoke,

but also other inhalable toxic substances can lead to the disease, whose point of origin is an inflammatory reaction of the pulmonary airways. Furthermore, COPD is closely linked with other diseases, such as heart disease or lung cancer (12,31).

1.2.2.1 Epidemiology

COPD is the most common chronic disease of the pulmonary system and it is the third leading cause of death worldwide. In 2014 about 63 million people suffered from the disease, which occurs more frequently in men than in women. In Germany, approximately 13% of all people older than 40 years suffer from the disease (12,31).

1.2.2.2 Aetiology

Without doubt, the leading cause of COPD is cigarette smoke. 90% of all patients suffering from COPD have smoked cigarettes in the past, but only 20% of all smokers will develop a COPD, which most likely can be lead back to genetic factors (12,19). Also, the smoking of other substances, such as cannabis or cigars, as well as passive smoking, plays an important role in the genesis of the disease. Still, there are many other factors that can cause COPD, including organic and inorganic dusts, chemical agents and fumes. Worldwide, many people use coal, wood or crop residues for heating in poorly functioning stoves, which leads to massive indoor pollution and is an underestimated risk factor for the development of COPD (32). In some cases, the appearance of COPD can be lead back to the profession. An association between pesticide use and the disease was shown already years ago and it could be observed that farmers, for instance, frequently develop a COPD (33). Also, people working in coal mines or as road builders, show an elevated risk to develop COPD. This can be explained by the inhalable noxes, which these occupational groups are often exposed to during work. If the disease occurs in patients younger than 50 years, endogenic factors should be considered, as for example α1 antitrypsin (AAT) deficiency (12). Research also showed that low birth-weight and severe respiratory infections during infancy, later on can be a decisive factor for suffering from COPD (33).

1.2.2.3 Pathogenesis

The inhaled particles, whether from cigarettes or other sources, provoke an inflammatory reaction of the small respiratory airways. At first, these inflammations

lead to a hypertrophy of the bronchial mucosa and a hyper secretion of mucus. Secondly, a remodelling of the respiratory epithelia can be observed and the clearing function of the microvilli and the kinocilia diminishes gradually. As a result, the overproduced mucus cannot be transported towards the pharynx and remains in the small airways. Ultimately, all these factors cause a severe bronchial obstruction (12,19,34).

Neutrophilic granulocytes and macrophages, located in the pulmonary interstitium and the pulmonary alveoli, produce proteolytic enzymes, called proteases. Because of the inflammatory reactions, the secretion of these proteases is increased. Normally, the proteases are counterbalanced by anti-proteolytic factors, like AAT, but due to the inhaled noxes, the anti-proteases partially lose their function (19). Furthermore, the amount of submucosal neutrophils increases with the intensity of smoking and also the number of macrophages correlates to the severity of COPD. The result is a proteolysis/anti-proteolysis imbalance, and as a consequence proteases begin to destroy the lung tissue (33). This, over time, leads to the development of pulmonary emphysema.

1.2.2.4 Symptoms

The two main symptoms of COPD are a severe cough with sputum production and an exertional dyspnoea, which increases with the progression of the disease. Both symptoms normally develop slowly and worsen over the years.

The productive cough can be explained by the elevated mucus production and the metaplasia of the respiratory epithelia. Because the mucus cannot be transported by the actual cleaning-systems of the lung anymore, the patients have to cough, trying to clear the bronchial airways that way (12). Typically, the productive cough occurs in the morning hours and many patients are symptom-free during the day. However, some patients may have symptoms also during night, keeping the patients from finding sleep (31).

Exertional dyspnoea can be lead back to the pulmonary emphysema and is therefore weakly developed at the beginning of the disease. Initially, it only occurs during exacerbations, which are defined as acute situations of symptom deterioration beyond normal day-to-day variations, which last for more than 24 hours and necessitate a change of medication. Exacerbations can be caused by bacterial and viral respiratory infects (80% of all cases) but also by indoor and

outdoor air-pollution, such as passive smoke (19,33). The following symptoms may be observed during an acute exacerbation: Gain of sputum production and cough, colour change of the sputum, severe shortness of breath, even when the patient is resting, and a general malaise (19). However, the longer the disease persists, the more frequent exertional dyspnoea appears and in the final stadium of COPD, it occurs constantly.
Most patients, suffering from COPD, also show systemic manifestations. It is assumed that extra-pulmonary manifestations origin in the lung but then disperse systemically.

The systemic manifestations, amongst others, include weight loss, osteoporosis, skeletal muscle dysfunction, anemia, diabetes, depression, cardiovascular diseases and malignancy. For example, 17% of all patients diagnosed with COPD, show a ventricular dysfunction (31).

1.2.2.5 Diagnosis

The first step for diagnosing COPD is a properly conducted anamnesis. The patient should be asked precisely about former or current smoking habits, as well as an exposure to other risk factors. Also, the pattern of the symptom development and the presence of extra-pulmonary comorbidities can give important information. As for diagnostic tools, pulmonary function tests have a high significant value. Spirometry tests should be performed in each patient to determine a potential airflow limitation, which is not only useful for diagnosing COPD, but also for therapy control. In patients with COPD, FEV_1 and FVC are diminished and the resistance of the airways is increased. Based on the severity of the airflow limitation, patients can be categorized into four different groups. The scheme has been released by GOLD (Global Initiative for Obstructive Lung Diseases) and is used worldwide. It is illustrated in Table 2.

Patients with $FEV_1/FVC < 70\%$:		
GOLD 1	Mild	$FEV_1 \geq 80\%$ predicted
GOLD 2	Moderate	$50\% \leq FEV_1 < 80\%$ predicted
GOLD 3	Severe	$30\% \leq FEV_1 < 50\%$ predicted
GOLD 4	Very severe	$FEV_1 < 30\%$ predicted

Table 2: GOLD classification of COPD, based on measured FEV_1 values

There are different validated questionnaires for patients, like the Modified British Medical Research Council (mMRC) questionnaire of breathlessness or the COPD Assessment Test (CAT). The goal of these tests is a subdivision of COPD patients.

Regarding the severity of their symptoms there are two main groups: “patients with mild symptoms“ and “patients with more severe symptoms”. By combining the results of the questionnaires with the previously demonstrated GOLD stadia, you will receive a combined COPD assessment, shown in the following figure:

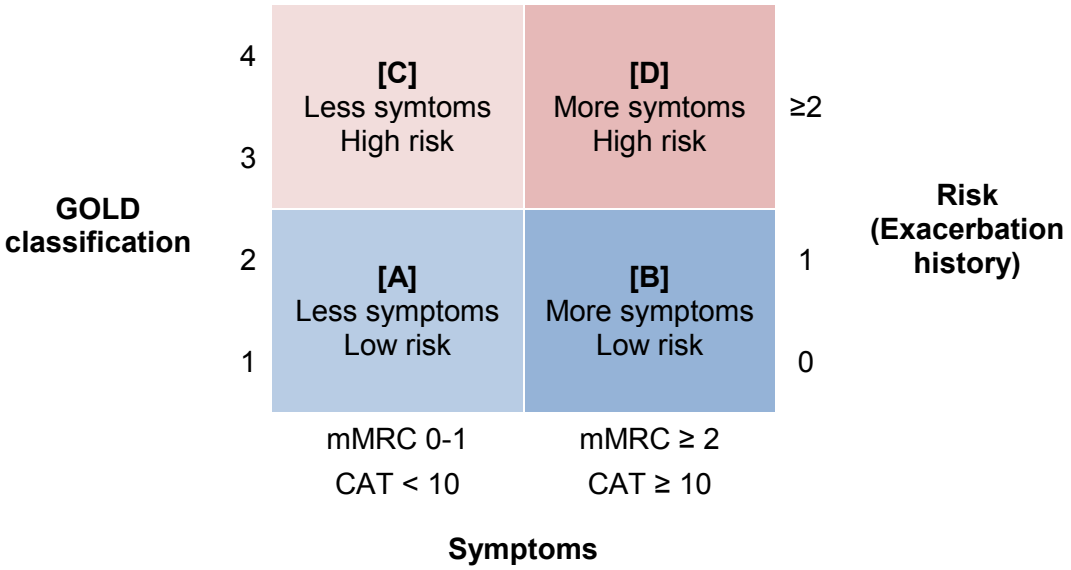

Figure 4: Combined Assessment for COPD. Modified from (35).

The combined COPD assessment has been established by GOLD (Global Initiative for Chronic Lung Disease) because FEV_1 alone is a poor descriptor of the disease status. It includes three different, highly important parameters of the disease and therefore reflects the complexity of COPD. As shown in Figure 4, the exacerbation risk of the patients is also a part of the combined assessment of COPD. It is based on the number and severity of exacerbations during the last year. The combined assessment test categorizes the patients into four different GOLD-groups: A, B, C or D. Based on this allocation, individualized treatment

guidelines for each group have been released, described in more detail in section 1.2.2.6 (12,32).

In many cases, to confirm the diagnosis of COPD, a bronchodilator reversibility test is done. If the FEV_1-value increases less than 15% or 200 ml, compared to the primarily measured value, COPD is very likely to occur. This test therefore can be helpful to differentiate between bronchial asthma and COPD.

In some cases, the symptoms of the diseases can be quite similar and therefore it can be difficult to make the right diagnosis. However, a main distinction of the diseases is that dyspnoea in bronchial asthma occurs as a sudden attack, whereas in COPD it develops slowly (19).

Blood examination is especially important during acute exacerbations. For example, the rise of inflammatory parameters, such as CRP (c-reactive protein), or a gain of leukocytes can indicate a fundamental infection. Furthermore, blood gas analysis gives information about the severity of the respiratory insufficiency. If COPD and/or pulmonary emphysema occur in young patients, the AAT-value should be dictated. Values lower than 90 mg/dl are highly suspicious for AAT deficiency syndrome (19).

Chest x-ray is a standard diagnostic tool, which is used as a matter of routine in COPD patients. A hyperinflation, an increased retrosternal airspace, flattened diaphragms and a “barrel chest” can be observed (31). However, the purpose of the chest x-ray is not to establish the diagnosis, but to exclude other possible diagnoses (32). For identifying and detecting pulmonary emphysema, computed tomography (CT) should be preferred, because it provides more detailed imaging of the lung parenchyma and a proper differentiation of the emphysema-type can be done (31).

1.2.2.6 Therapy

The main goals of COPD treatment include an improvement of current symptoms and a risk reduction of future events, such as exacerbations and disease progression.

The therapy of COPD also includes non-pharmacological treatments, like pulmonary rehabilitation. It is a multidisciplinary programme, where patients learn about their disease plus its consequences and different physical exercises.

Studies showed that physical exercise has a significant impact on the disease and patients, who maintain physical activity, have less exertional dyspnoea and a better quality of life. However, smoking cessation is by far the most important intervention in COPD treatment. It is essential to completely quit smoking, but for many patients this may be a very challenging task.

For this reason, patients should be encouraged continuously and the use of pharmacological substances, like for example varenicline, a partial agonist of the nicotinic receptor, should be considered at an early stage. Furthermore, vaccinations against pneumococcus and influenza should be considered in each patient to reduce respiratory infections and acute exacerbations. Additionally, influenza vaccinations may minimise the mortality rate (31,36).

Regarding the pharmacological treatment of stable COPD, many different guidelines have been released. The most commonly used tough, is the GOLD-guideline, which gives treatment recommendations referring to the different GOLD-groups, demonstrated in Table 2.

Patients with few symptoms and a low risk of exacerbations, who therefore belong to group A, initially should be treated with short-acting, inhalable beta agonists, only in case of need. However, if the airflow limitation is more severe, a combination of different SABAs or the additional use of long-acting beta agonists should be considered.

Patients belonging to group B show more severe symptoms but still a low exacerbation risk. The pharmacological treatment should be started with LABAs. Short-acting bronchodilators can be taken additionally when needed. If no improvement can be achieved, a combination of different LABAs can be administered, but patients receiving this combined therapy should be followed up accurately. Another possibility is the combination of SABAs and theophylline.

Group C patients have few symptoms but a high exacerbation risk. The initial treatment should include either a therapy with a long-acting anti-cholinergic substance or a combined ICS/LABA therapy. Both of the long-acting substances will reduce the exacerbation risk. In cases, where LABAs are not available or too expensive, the previously mentioned combination of SABAs and theophylline should be used.

Group D includes all patients suffering from severe symptoms and showing high exacerbation risks. The initial treatment is the same as for group C patients. However, for this group it is especially important to avoid noxes, which may lead to exacerbations. Therefore, the non-pharmacological treatment has a high value in this group.

Furthermore, if the initial therapy does not lead to amelioration, in some cases a combination of ICS, LABAs and long-acting anti-cholinergics can be administered. If the patient has chronic bronchitis, a phosphodiesterase-4-inhibitor (PDF-4-inhibitor) can be added to the treatment plan. This is also valid for group C patients. It is most effective, when combined with LABAs. To achieve the best possible therapy, follow ups should be done regularly in each patient group.

Patients suffering from an acute exacerbation need an intensified therapy because exacerbations can be lethal and have to be treated at an intensive care unit. Bronchodilators, corticosteroids and antibiotics are the most effective substances when treating AECOPD (acute exacerbation of COPD). Regarding corticosteroids, oral substances are preferred and normally a dose of 30-40 mg prednisolone for 10-14 days is administered. Studies showed that corticosteroids have positive effects on lung function (FEV_1), arterial hypoxemia and can reduce the recovery time. SABAs are used to reduce bronchial obstruction and therefore deliver a rapid amelioration of the symptoms. In most cases, SABAs are already included in the therapy scheme, why the drug dose has to be increased to achieve results.
Antibiotics should be given to all patients, when a bacterial infection is assumed. Increased sputum amount, greenish colour of sputum and impaired dyspnoea often are decisive symptoms. Placebo-controlled studies showed that antibiotics reduce the short-term mortality, treatment failures and sputum purulence. In general, the choice of the antibiotic should always be based on an antibiogram, but in some cases the treatment has to be initiated before receiving results. In this case, antibiotics, which are also effective against gram-negative bacteria, should be preferred. If acute exacerbations occur, blood gas analysis should be performed to determine respiratory insufficiency and decide whether a patient needs temporary oxygen therapy (19,32).

Patients suffering from very severe symptoms and showing values of PaO_2 <50 mmHg in rest (<60 mmHg if patients additionally suffer from cor pulmonale) need a permanent oxygen therapy.

A therapy at home can be considered if the patient is still mobile and reduced PaO_2 values occur mainly during exertion. Otherwise, the oxygen therapy has to be administered in hospital. If $PaCO_2$ values increase under the therapy and patients show signs of mild CO_2 intoxication, like headache or sleepiness, the therapy has to be adapted and O2 should be administered only during night.

In the final stadium of the disease, when patients show distinctive emphysema, surgery can be an option. During bullectomy, large bullae, which do not contribute to gas exchange, are removed and therefore other lung sections are decompressed. In a lung volume reduction surgery (LVRS), whole parts of the lung are removed, often bilaterally. As a last, life-saving option in end-stage COPD, lung transplantation can be considered (19,36).

Concluding it is important to mention that not only COPD has to be treated, but also comorbidities. These diseases often have a very high impact on the prognosis and sometimes even represent the life determining factor (32).

1.2.3 Asthma COPD overlap syndrome (ACOS)

Although definitions of ACOS vary, it is clinically described as a persistent airflow limitation in patients, who show features of bronchial asthma and COPD. This definition was released by GINA and GOLD in 2014. Over the last few years, ACOS has gained a lot of attention because it is widely spread - it affects about a quarter of patients, who suffer from COPD, and almost a third of patients who previously had bronchial asthma. Patients with ACOS have significantly worse respiratory symptoms, a poorer quality of life and an increased risk of exacerbations than patients who suffer from asthma or COPD alone, indicating that ACOS is an independent phenotype in the airways disease spectrum and may have its own clinical appearance. However, it is still uncertain, whether ACOS is merely an evolution from longstanding COPD or asthma or is its own disease entity with a unique pathogenesis. This lack of knowledge has also limited the discovery of ACOS specific treatments. Furthermore, patients with ACOS are often overlooked or excluded in clinical trials investigating novel treatments for bronchial

asthma and COPD. As a result, it can be extremely difficult for clinicians to identify and treat patients with ACOS. The investigation of this group of patients is highly important (37,38).

1.3 Anti-obstructive medication

In general, there are three groups of anti-obstructive medication: bronchodilators, like beta-2 agonists, muscarinic antagonists and methylxanthines. They act by different mechanisms, as shown in Figure 5, and have different indications.

Methylxanthines inhibit different enzymes of the phosphodiesterase (PDE) enzyme family and this, as a result, leads to higher concentrations of intracellular cAMP (cyclic adenosine monophosphate). The increase of cAMP then causes, amongst others, a relaxation of the smooth muscles. Furthermore, methylxanthines can also inhibit adenosine receptors on the surface of cells. Adenosine normally causes a contraction of smooth muscles in the airways and the release of histamine from airway mast cells. However, the use of methylxanthines, such as theophylline and aminophylline, is restricted to acute exacerbations.

Beta-2 agonists and muscarinic antagonists can be short-acting (SABA and SAMA) and long-acting (LABA and LAMA), depending on the compound. Muscarinic antagonists, also known as parasympatholytic drugs, block muscarinic receptors. Both smooth muscle and secretory glands of the small airways in the lung receive vagal innervations and therefore show muscarinic receptors. The administration of atropine, which represents the classical anti-muscarinic drug, causes a blockade of the cholinomimetic action at muscarinic receptors. This results in a bronchodilatation of the airways and furthermore reduces the secretion of mucus. However, anti-muscarinic drugs are still not as useful as beta-2 agonists regarding the treatment of asthma patients, but ipratropium and tiatropium, which are synthetic analogues of atropine, are often used in patients who suffer from COPD.

To reduce systemic side effects, these substances are administered via inhalation. Ipatropium is a short-acting drug, whereas tiatropium is categorized as long-acting muscarinic antagonist with a terminal elimination $t_{1/2}$ of 5-6 days. It has been shown that tiatropium reduces the incidence of COPD exacerbations (39).

The short-acting beta agonists will be described in more detail in the following section.

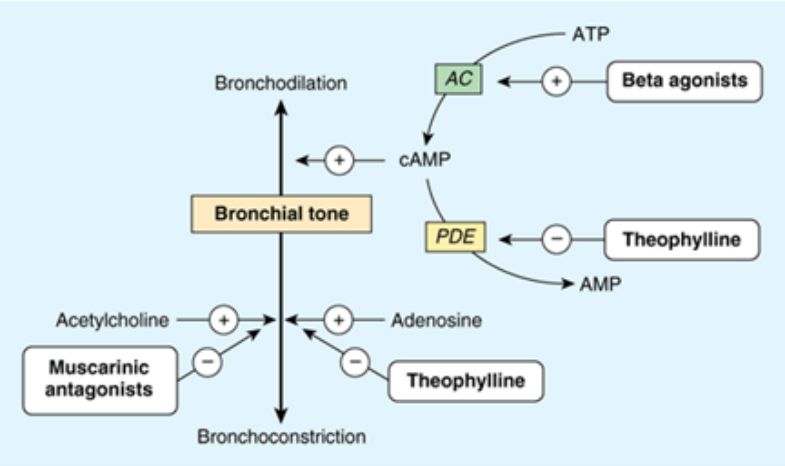

Figure 5: Mechanisms of different anti-obstructive drugs (39)

1.4 Short-acting beta agonists

Short-acting beta agonists, abbreviated as SABAs, represent an important pharmaceutical agent regarding the treatment of bronchial asthma and COPD. The most common used agents are albuterol, fenoterol and terbutalin.

All of these substances have a bronchodilating effect, which starts a few minutes after the drug intake and lasts for approximately 3-5 hours. The substances in general are administered as inhalable formulations, either via metered-dose inhalers (MDIs) or dry powder inhalers (DPIs).

SABAs release its effect via activating $ß_2$ adrenergic receptors. By binding to the receptors, different enzymatic cascades are activated which, in the end, lead to a smooth muscle relaxation and therefore bronchodilatation. More precisely, the binding causes the activation of adenylyl cyclase and this step on the other hand causes an elevation of cAMP, which in turn will activate the protein kinase A and lead to smooth muscle relaxation (40).

However, ß2 receptors are not only located in the respiratory airways and therefore SABAs can cause extrapulmonary side effects, such as peripheral vasodilatation, which results in tachycardia. Furthermore, an increased insulin release and a relaxation of the uterine muscle can occur. Due to the last fact, SABAs should be administered carefully during pregnancy (41–43).

1.5 Particle deposition in the lung

The prerequisite for a therapeutic action of the afore mentioned drugs is the deposition of the drug particles in the lower airways. The most crucial factor for this deposition process is the particle size. It is well known that only particles with an aerodynamic diameter between 1 and 5 µm can reach the last instances of the lung. Studies showed that particles larger than 5 µm impact in the upper airways and particles smaller than 1 µm will be exhaled by the patient (7). Depending on the particle size, there are three main deposition mechanisms: Impaction, sedimentation and diffusion (Figure 6).

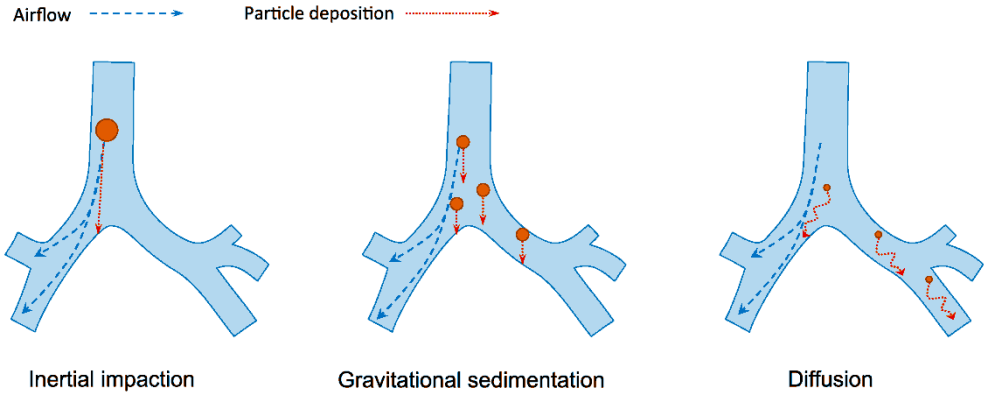

Figure 6: Mechanisms of particle deposition in the lung (44)

Impaction only affects large particles, which show diameters above 5µm. Because of their size and their inertia, these particles are likely to impact on the walls of the upper airways and then are swallowed by the patient.

Sedimentation, which typically occurs in particles with a diameter between 1 and 5 µm, describes the deposition of particles due to gravity and can be described with Stokes' law for sedimentation. The sedimentation velocity is highest in particles with large diameters and great density.

Diffusion concerns particles with an aerodynamic diameter <1 µm. These particles are influenced by the Brownian motion of the encircling gas particles and therefore can only be deposited via diffusion. The diffusion velocity is inversely proportional to the aerodynamic diameter (7).

1.6 Particle synthesis

In order to generate small, inhalable sized particles, different techniques are available. The most common one is milling the active pharmaceutical ingredient (API) to the required size. As an alternative, spray drying can be used. The processes will be described in more detailed in chapter 2.2.1 and 2.2.2. Both techniques lead to inhalable sized particles but important properties of the generated particles, like shape and solid-state, can vary. For example, milling normally keeps the needle-like shape of the drug crystals, whereas spray drying creates spherically shaped particles.

1.7 Inhalation therapy and different inhalers

The use of inhalable drugs in the treatment of respiratory diseases is associated with many advantages over oral and parenteral routes of delivery. The administration is painless, a reduction of systemic side effects can be observed and most inhalable drugs show rapid onset of action. Additionally, the direct deposition of the drug in the lung leads to in higher local drug concentrations for much lower doses compared with a systemic administration.

To apply inhalable drugs, inhaler devices are used. There are many different systems on the market, such as dry powder inhalers (DPIs), pressurized metered-dose inhalers (pMDIs) or nebulizers. Each system has specific advantages and disadvantages and the choice of which system to use should be made individually for each patient, since it depends on many factors. Table 3 gives an overview of advantages and disadvantages of the different systems.
As a rule of thumb, children and infants (≤4 years) are treated with nebulizers, which are also used for the treatment of acute symptom episodes.

Deposition in the gastrointestinal tract is lowest for nebulizers and deposition in the apparatus is highest. The control of obstructive lung diseases in adults is mainly achieved by pMDIs or DPIs, which show higher deposition in the gastrointestinal tract but lower deposition in the apparatus. The choice between DPI and MDI is mainly driven by patient's parameters (e.g. inspiratory flow and coordination). More precisely, in DPIs the drug is delivered as a dry powder and the energy to disperse the powder during inhalation relies on the patients inspiratory flow rate. Due to this, patients, who suffer from a severe airflow limitation, often may not be

able to properly use DPIs. Nebulizers and pMDIs use liquid formulations. The difference between these two systems is that nebulizers use an external energy source to produce aerosolized fine particulate droplets of the formulation, while pMDIs incorporate a propellant into the formulation, which provides the energy for aerosolization upon actuation. Currently, most medications for local lung therapy are applied by pMDIs, but the market of DPIs is increasing (45–47). Figure 7 shows different dry powder inhalers, which are currently available on the market.

Inhalation device	Advantages	Disadvantages
Nebulizers	No specific inhalation technique required Aerosolizes most drug solutions Delivers large doses Suitable for infants and children <4 years	Time consuming Non portable Contents easily contaminated Relatively expensive Poor delivery efficiency Drug wastage
pMDIs	Compact Portable Multidose (approximately 200 doses) Inexpensive Reproducible dosing	Inhalation technique required High oral deposition Maximum dose of 5mg Limited range of drugs available Dependent on inspiratory flow rate Humidity may cause powder aggregation Most DPIs containe lactose
DPIs	Compact Portable Breath actuated Easy to use	

Table 3: Advantages and disadvantages of different inhaler devices. Modified after (46).

In all powder inhalers, the API has a powder formula. The small API-particles are attached to the surface of larger carriers, which show diameters ranging from 50–200 µm. These carrier-based formulations are necessary to improve the flowability of the API, which would be highly unsteady without carriers due to the cohesive properties of the small, powdery API-particles. As a result, carriers improve dosing accuracy and minimize the dose variability. There are different substances that can be used as carriers but most frequently they are represented by α-lactose monohydrate. It is important to mention, that the API has to detach from the carrier in the upper airways, so that only the API reaches the lower airways and can execute its function. The detachment process is influenced by the force of the

patient's inspiration and the velocity of airflow – the more powerful the inspiration, the more likely is a detachment of API and carrier. The patient's collaboration and inhalation technique has a high impact on the efficacy of inhalable drugs. Studies showed that errors in the inhalation technique occur in 20-80% of all patients. Therefore, it is necessary to show each patient how to use their inhalers appropriately (7,47,48).

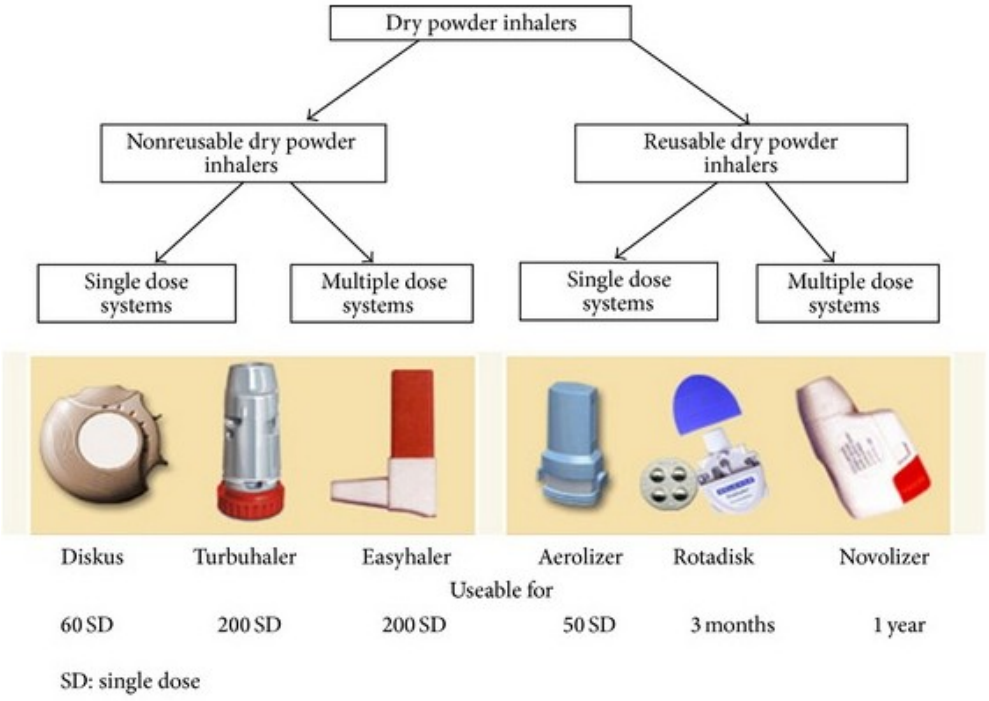

Figure 7: Different dry powder inhalers (49)

1.8 Aim of the study

As mentioned above, different API processing techniques, such as jet-milling or spray drying, can lead to differences in shape and solid-state of the generated particles. Previous studies showed that for salbutamol sulphate, these different properties will lead to different results concerning in-vitro lung deposition, which can be determined with NGI-experiments (Next Generation Impactor). Salbutamol sulphate was chosen as a model drug because it is a frequently used drug to relieve obstructive symptoms in pulmonary diseases. Consequently, this study aims to test whether the differences in particle properties also impact biological interactions with lung cells. The particle shape, spherical versus needle shaped, is the key parameter investigated as macrophages are expected to ingest rod like structures to a higher extent than spherical particles. Therefore, the API primarily was modified through jet-milling and spray drying and particle properties like size, shape and solid-state were determined. Afterwards, permeability-tests and cellular uptake experiments with different cell-types were performed. Namely, Calu-3 and A549 cells were used as representatives of bronchial and alveolar epithelial cells, respectively DMBM-2 murine macrophages as model for alveolar macrophages. Furthermore, adhesive mixtures were prepared with jet-milled and spray dried salbutamol sulphate and α-lactose monohydrate as model carrier. These formulations were filled manually into capsules and dissolution tests, coupled with NGI experiments, were performed.

2 Materials and Methods

2.1 Salbutamol Sulphate

Salbutamol sulphate, also known as albuterol sulphate, represents the API which has been used for this study. The substance in USP25 quality was purchased from Selcetchemie AG (Zurich, Switzerland).

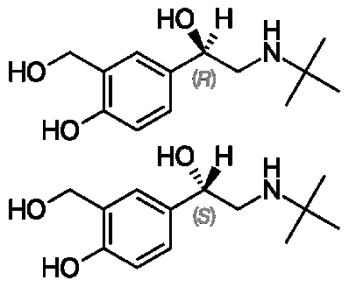

Figure 8: Different racemic structures of salbutamol sulphate

Salbutamol sulphate is a white, crystalline solid. It is prepared as a racemic mixture of R(-) and S(+) stereoisomers, shown in Figure 8 (50).

2.2 Modifying of the API

For creating particles of inhalable sizes, two different methods were used.

2.2.1 Jet-milling

Jet-milling is a commonly used process to create inhalable sized particles with an aerodynamic diameter ranging from 1-5 µm. During the process the raw material is reduced by collision of particles induced by high-pressure air or nitrogen fed through the nozzles.

In the present study, the modification of the API was performed with an air jet mill (Spiral Jetmill 50 AS, Hosokawa Alpine AG, Augsburg, Germany), shown in Figure 9. An injection pressure of 6 bar and a milling pressure of 3 bar were used. The powder feeding was done manually.

Figure 9: Hosokawa Spiral Jetmill 50 AS

2.2.2 Spray drying

The second method, which was used to create inhalable sized particles, was spray drying. Spray drying is a method to produce a dry powder from a solution or suspension by rapidly drying it with a hot gas. The liquid input stream is sprayed through a nozzle into the spraying tower and vaporized. Passing the drying chamber, moisture quickly leaves the droplets resulting in dry, solid particles that can be collected on the bottom of the drying chamber.

Before starting the spray drying process, aqueous solutions of salbutamol sulphate and purified water, with a salbutamol sulphate concentration of 7.5%, were prepared. The solutions were prepared directly before starting the spray drying process. Purified water was taken from “TKA MicroPure UV UltraPure Water System” (TKA Wasseraufbereitungssysteme GmbH, Niederelbert, Germany).

As for the spray dryer, the following model was used: Nano Spray Drier B-90 (Buchi Labortechnik AG, Flawil, Switzerland). It is illustrated in Figure 10.

Figure 10: Buchi Nano Spray Drier B-90

The spray drier was equipped with the long version of the drying chamber. A mesh of 7 µm was used to create inhalable sized particles. The spray drier was fed with the 7.5% concentrated solution using the following conditions:

- Inlet temperature: 120°C
- Flow: 110 l/h
- Pressure: 36 mbar

- Spray intensity: 30%

After the spray drying process, the powder was collected from the collection electrode and then stored in a dessicator over silicia gel at room temperature.

2.3 Preparation of adhesive mixtures

For NGI experiments and dissolution testing, two 10 g mixtures of Lactohale 100 (LH100) and the primarily modified APIs were prepared. The API content of the mixtures was 2%. For preparing the blends, a sandwich method was used. More precisely, half of the needed LH100 was layered in a metallic vessel, then the calculated amount of API was added and lastly the remaining part of LH100 was added to the vessel. The two substances then were mixed with a tumble blender (T2F Turbula®, Willy A. Bachhofen AG Maschinenfabrik), using the following mixing conditions:

- Mixing for 60 minutes at 62 rpm (revolutions per minute)
- Milling the blend through a 400 µm sieve
- Final mixing for 60 minutes at 32 rpm

As mentioned in the introduction, carriers in dry powder formulations most frequently are represented by α-lactose monohydrates. Lactose is a natural disaccharide and a condensation product of galactose and glucose.

Lactohale 100 (DFE Pharma, Goch, Germany) comprises of α-lactose monohydrate and is a commercially available standard carrier for inhalation products. The particles are crystalline, have a tomahawk-like shape with a smooth surface and a mean particle size of about 100 microns (51).

After the preparation of the two different mixtures (LH100 + spray dried SS and LH100 + jet-milled SS), the mixing homogeneity was determined. Therefore, 10 samples of approximately 250 mg were taken from each mixture with a spatula. More detailed, 3 samples were taken from the top of the blend, 4 samples from the middle and the last 3 samples from the bottom. The samples then were dissolved in 100 ml of buffer. For the buffer, purified water was adjusted to a pH of 3, using acetic acid.

The samples were put into the ultra-sonic bath for approximately 5 minutes and afterwards the salbutamol sulphate concentration of each sample was determined

using reversed phase HPLC (high performance liquid chromatography). The homogeneity of the blends was expressed as the coefficient of variation of the drug content of n=10 samples.

2.4 Particle characterisation

As already mentioned, studies showed that different methods of modifying particle size can lead to different particle properties. In order to determine particle properties and characteristics, different methods were used. In general, all experiments performed for particle characterisation were done in triplicate.

2.4.1 Laser diffraction

Laser diffraction (HELOS/KR, Sympatec, Clausthal-Zellerfeld, Germany) was used to determine particle size and particle size distribution. Laser diffractometers, in general, interpret light scattering patterns from solid particles or liquid droplets in a collimated beam of coherent light (52). The different powders were dispersed using a dry dispersing unit (Rodos/L, Sympatec, Clausthal-Zellerfeld, Germany) and a vibrating chute (Vibri, Sympatec, Clausthal-Zellerfeld, Germany). The dispersing pressure was 2 bar. The collected data was analysed with the Windox 5 software (Sympatec). Using this technique, three characteristic particle diameters were determined: x_{10}, x_{50} and x_{90}.

2.4.2 Small and wide angle x-ray scattering (SWAXS)

Small and wide angle x-ray scattering was used to determine the solid-state of the powder particles. It gives information about the distribution, the size and the shape of macromolecules. SWAXS is a technique, where x-rays are scattered by an inhomogeneous sample in the nanometre-range at wide angles (>5°) and small angles (typically 0.1-5°). Small angle x-ray scattering (SAXS) normally delivers structural information of molecules between 1 and 200 nm.

Wide angle x-ray scattering (WAXS) can measure samples between 0.33 nm and 0.49 nm (53). The WAXS measurements were performed with Microcalix (Bruker AXS, Karlsruhe). An exposure duration of 600s was chosen and the samples were analyzed at 25°C, 120°C, 170°C, 200°C and after 30min again at 200°C.

2.4.3 Differential scanning calorimetry (DSC)

DSC 204 F1 Phoenix (Netzsch, Selb, Germany) was used to analyse the glass transition temperature of the samples. The thermograms give information about the thermal behaviour and the corresponding solid-state of different particles. Prior to the measurements, 3-5 mg of the samples were put into hermetically sealed pans. For the weighing of the samples, a high precision scale (XP205DR, Mettler Toledo GmbH Vienna, Austria) was used. During the DSC measurements, the samples were heated from 25°C to 230°C, using a heating rate of 5°C/min. For the evaluation of the thermograms the Netzsch Proteus Thermal analysis software, version 6.1.1 (Netzsch, Selb, Germany) was used.

2.4.4 Scanning electron microscope (SEM)

A scanning electron microscope was used to analyse the morphology and the particle structure of the modified APIs and the different blends. The microscope used was a Zeiss Ultra 55 (Zeiss, Oberkochen, Germany). The samples were gold palladium sputtered prior to analysis and the operating energy was 5 kV. All SEM images in this work were taken at FELMI (Austrian Center for Electron Microscopy and Nanoanalysis, Graz, Austria).

2.5 Testing of the aerodynamic performance

For testing the aerodynamic properties of the particles, a next generation impactor (NGI, Copley Scientific, Nottingham, United Kingdom) was used. Impactors, as described in the Pharmacopoeia, represent an artificial lung and therefore in-vitro lung performances of different substances can be evaluated.

The NGI is a multistage cascade impactor. An airflow passes through the impactor in a saw tooth pattern and the velocity of the air stream is successively increased by forcing it through a series of nozzles, which show progressively reducing jet diameters. By increasing the airstream, particle separation and sizing can be achieved: larger particles will follow inertia and deposit and smaller particles will reach the next impactor stage.

During the experiments the aerosol is discharged from the inhaler and, because of the airflow, sucked through the whole impactor. The powder formulation then is collected in a series of collection cups and consequently the amount of API, deposited in each stage, can be quantified via HPLC.

Various important parameters for characterizing DPI formulations can be received from NGI experiments. The mean dose delivered and the delivered dose uniformity are important parameters regarding the development of new formulations. They are used to guarantee the quality and efficacy of newly developed formulations.
Furthermore, according to the European Pharmacopoeia (preparations for inhalation, Ph. Eur., 7.0), the fine particle dose (FPD) and the emitted dose (ED) can be calculated. The FPD depicts the amount of API with an aerodynamic diameter below 5 µm. The ED represents the total amount of API, which has been collected from all stages of the impactor.
Additionally, the fine particle fraction (FPF) can be determined. It is defined as the percentage of relative to total mass (FDP/ED), and represents the percentage of API-particles, that have been separated from the carrier and show aerodynamic diameters below 5 µm. As already mentioned, all particles having an aerodynamic particle size smaller than 5 µm, can reach the deep lung. Consequently, the FPF is the main parameter for characterizing the performance and the efficiency of a DPI carrier system. In addition, the FPF is by far the most common parameter to compare the performance of different DPI formulations among each other.
The MMAD (mass median aerodynamic diameter) is defined as the diameter at which 50% of the particles by mass are larger and 50% are smaller. This governs the respirable fraction and represents the particle deposition pattern in the lungs.

In general, the NGI consist of different parts: the lid, the seal body, the different nozzle pieces, the collection cups, a cup tray and the bottom frame. However, to perform NGI experiments, a pre-separator, an induction port and a mouthpiece adapter were attached to the NGI. The induction port has a right-angled shape and represents the human throat. The mouthpiece was used to attach a suitable inhaler and the pre-separator is important for capturing large particles.
By connecting the NGI to a vacuum pump (SV1040, Busch, Chevenez, Switzerland), the airflow through the NGI was guaranteed. Figure 11 illustrates the fully assembled NGI.

Figure 11: Fully assembled NGI

The setting conditions of the NGI and the procedure of the experiments were based on the European pharmacopoeia.

Preliminary to the experiments, the cups of the NGI were coated with 2% Tween in ethanol and stored under the hood until they were dried. The vacuum pump was turned on 30 minutes before starting NGI experiments. The NGI then was fully assembled and 10ml of buffer (purified water and acetic acid with a pH-value of 3) were added to the pre-separator. As NGI experiments and dissolution experiments, which will be described in section 2.6, were performed successively, stage 2, 3 and 4 were equipped with an impaction insert for dissolution testing. For all experiments, Aerolizer® devices (shown in Figure 12) were used and the capsules were filled manually with approximately 25 mg of the two different blends.

During each experiment, 6 capsules were used consecutively to reach a detectable amount of API. In general, NGI and dissolution experiments were repeated 4 times (n=4).

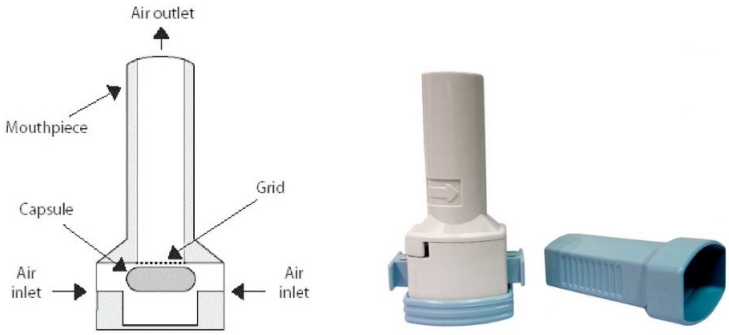

Figure 12: Illustration of the Aerolizer® device (54,55)

As the Aerolizer® is a low resistance inhaler, a flow rate of 100 ml/min was adjusted. By choosing an opening time of the solenoid valve of the critical flow controller (TPK, Copley Scientific, Nottingham, United Kingdom) of 2.4 seconds, an airflow of 4 l/min was guaranteed. This reflects the average amount of airflow during inhalation in adults. Before starting the NGI experiment, the assembling of the impactor and its tightness were checked by performing a leak test. The solenoid valve was opened and the mouthpiece was sealed with a plastic stopper. During 60 seconds, the pressure must not increase more than 2 kPa. Lastly, the P_3/P_2 quotient was calculated – values higher than 0.05 kPa, may indicate that the vacuum pump is too weak.

Six capsules, which had been filled before, were put sequentially into the same device. Before opening the solenoid valve, each capsule was pierced manually by pressing two buttons on the outside of the device. This step guarantees a sufficient release of the blend inside the capsule. The solenoid valve was opened five times consecutively for each capsule for 2.4 seconds. By opening the solenoid valve, air is sucked through the impactor, followed by powder discharging into the impactor.

The NGI then was disconnected from the vacuum pump and the critical flow controller was turned off. For receiving samples for HPLC analysis, the NGI was dissembled and its different stages were rinsed with a specific amount of buffer. The inhaler device was rinsed with 10 ml of buffer.

The mouthpiece and the induction port of the NGI were rinsed with 10 ml of buffer into the same glass beaker. Regarding the pre-separator, an amount of 50 ml was used and the collection cups in general were rinsed with 10 ml of buffer, except for stage 2, 3, and 4, which were used for dissolution testing and therefore will be described separately in chapter 2.6.
The samples were transferred into vials and the salbutamol sulphate concentration of each stage was measured with HPLC.

2.6 Dissolution

Inhalable drugs, in general, layer themselves onto the lung lining fluid after inhalation and therefore have to dissolve in the lung fluid for being efficient. The dissolution rate determines the pulmonary residence time of the drug and

therefore represents an important parameter concerning pulmonary targeting. There are different techniques for dissolution testing, but a standardized method has not been proposed yet (56). In our case, dissolution testing was performed corporately with the NGI experiments, respectively directly after the NGI experiments, using a modified, more physiological set up with lower volumes instead of the standard dissolution apparatus and method.

Initially, simulated lung fluid (SLF) was prepared, using the following materials:
PBS, 1,2-Dipalmitoyl-sn-glycero-3-phosphocholine (DPPC) (TCI Deutschland GmbH, Germany), absolute ethanol (Sigma Aldrich, Germany). For the DPPC stock solution 39 mg DPPC were weighed in with a high precision scale and added to 3 ml ethanol. The DPPC stock solution was then added slowly and carefully to 195 ml of preheated buffer (approximately 37°C) while stirring. The slightly turbid solution then was put into the ultra-sonic bath for approximately 20 minutes at 37°C.
Preparing the dissolution testing, 55 ml of the SLF were added to crystallizing dishes with a volume of 250 ml, which then were placed onto a laboratory shaker. The temperature was set to 37°C and a rpm of 60 was chosen. The rest of the SLF was kept in a glass beaker and also placed on the laboratory shaker for later use.

As already mentioned above, stage 2, 3 and 4 of the NGI were adjusted with the impaction insert. After performing the NGI experiment, as described in chapter 2.6, the impaction inserts were removed from the NGI cup. A membrane, which had been pre-soaked with SLF, was put on top of the inserts and sealed in place with the securing ring of the membrane holder. Each of the 3 sealed membrane holders then was placed separately into the dissolution vessels on the laboratory shaker. Directly after placing the membrane holders into the vessels, the first sample (time: 0 minutes) was taken. A sampling-volume of 500 µl was chosen and the samples were taken after 0, 2, 5, 10, 20, 40, 60, 120 and 180 minutes. Whenever a sample was taken, 500 µl of SLF were added to the dissolution vessel to keep the total volume stable. The samples were transferred directly into HPLC vials and the salbutamol sulphate concentration was measured using HPLC. In between the sample-taking, the impaction inserts, from which the membrane holder had been

removed before, were rinsed with 10 ml of buffer and samples were filled into HPLC vials for measurement.

2.7 Cell culture

2.7.1 Cultivating the cells

Cell cultivation in general means, that cells are transferred into sterile culture flasks and a specific culture medium is added. Due to this, the cells can grow outside an organism, using the culture medium as nutritive substance. The cell culture flasks are stored in an incubator with a specific CO_2 concentration and specific temperature conditions. When the entire bottom of the flask is covered by cells, they will stop to grow and inhibit each other's proliferation. Because different cell-types grow with variable velocity, it is highly important to control the cell growth frequently, using specific inverted microscopes for cell culture. If the cells are growing adherent and cover approximately 80% of the flask bottom, splitting of the cells should be performed (2.7.2: Subculturing of the cells). Furthermore, it is important to mention, that the culture medium has to be changed approximately every second day.

All cells were manipulated under aseptic conditions using Herasafte^{TM} KSP class II Biological Safety Cabinet (Thermo Scientific, Thermo electron GmbH, Mannheim, Germany) to prevent a contamination of the cells. Furthermore, aseptic equipment was used for the experiments and all media or solutions were pre-warmed to 37°C prior to use.

Calu-3 cells: The cells derived from a human adenocarcinoma of the lung, can produce mucus and form tight monolayers (57). Calu-3 cells were obtained from the American Type Culture Collection (ATCC, HTB-55, LGC Standards GmbH, Wesel, Germany).

The cells were cultured in 175 m^2 cell culture flasks (Greiner Bio-One GmbH, Rainbach, Austria), using 90% Minimum Essential Medium (MEM) with Earle's salt, 10% fetal bovine serum (FBS), 2 mM L-glutamine and 1% penicillin-streptomycin. It was provided by Life Technologies (Vienna, Austria). The cells were cultured at 37°C in humidified air containing 5% CO_2 (Galaxy R CO_2 Incubator, RS Biotech, Scotland, Great Britain).

A549 cells: This cell line derived from an adenocarcinoma of a human lung. Because the cells form confluent monolayers with type II alveolar cell characteristic morphology, A549 cells represent a standard in-vitro model for type II alveolar cells and are often used to study pulmonary toxicity (58). The cells were obtained from Deutsche Sammlung für Mikroorganismen und Zellkulturen GmbH (Braunschweig, Germany).
A549 cells were also cultivated in 175 m^2 cell culture flasks but a different culture medium was used. It contains 450 ml DMEM (Dubeccos Modified Eagle Medium, provided by Life Technologies, Vienna, Austria), 10% FBS, 2mM L-glutamine and 1% penicillin-streptomycin.

DMBM-2 cells: These cells are macrophages, which derived from the bone marrow of a mouse. DMBM-2 cells are round cells, which grow in loose aggregates and do not form tight junctions. The cells were obtained from Deutsche Sammlung für Mikroorganismen und Zellkulturen GmbH (Braunschweig, Germany) and cultured in DMEM, supplemented with 80% RPMI 1640, 20% horse serum, 1mM sodium pyruvate, 1mM non-essential amino acids, 1,25 µg/ml vitamin B12, 2mM L-glutamine and 1% penicillin-streptomycin (provided by Life Technologies, Vienna, Austria).

2.7.2 Subculturing of the cells

If cell proliferation is inhibited because the cells cover the entire bottom of the culture flask, a specific number of cells has to be transferred to a new cell culture flask. In this manner, the growth of the cells can be guaranteed. For subculturing, the following steps were performed:
Initially, the culture medium was removed with a Pasteur pipette. The cells then were washed with approximately 10 ml of PBS buffer to remove residues of FBS. Afterwards, 2 ml of a 0.05% concentrated Trypsin-EDTA solution were added to the culture flask and distributed evenly on the surface of the flask by swirling the flask gently. Trypsin is responsible for detaching the cells from the surface of the culture flask. EDTA (Ethylenediaminetetraacetic acid) is a Ca^{2+} chelator and loosens the junctions between the cells. The flasks then were put into the incubator (5% CO_2, 37°C) for a specific time. DMBM-2 cells normally don't form tight junctions and due to this, the incubation time was only a few minutes (2-3 minutes). A549 cells and Calu-3 cells had to rest in the incubator for approximately

10 minutes because they form more adhesive layers. Using an inverted microscope (Olympus CKX41, Olympus Austria GmbH, Wien, Austria), the condition of the cells was checked and it was possible to determine, if the cells were already in suspension or not. The detaching process can be facilitated by tapping carefully to the outer side of the flask. As soon as all cells were detached, 10 ml of fresh culture medium was added to the culture flask, spreading it on the whole surface of the flask, to inhibit further trypsin reaction. The cells then were suspended thoroughly by pipetting the medium slowly up and down. The 12 ml cell-medium solution inside the flask then was transferred into a 15 ml falcon tube. Depending on which dilution was chosen, a specific amount of the cell-suspension was transferred to a new culture flask and new culture medium was added to guarantee cell growth. Trypsin-EDTA solution and PBS were provided by Life Technologies (Vienna, Austria).
The cells then were centrifugalized for 5 minutes at 800 U/min (Heraeus Biofuge Fresco).

Afterwards, the supernatant was removed with a pipette, making sure not to damage the cell-pellet at the bottom of the falcon. New culture medium was added to the falcon, to be specific the same amount that has been removed, and the cells were resuspended using the pipette.
Prior to seeding the cells, the cell number had to be determined. This was performed with a Casy® cell counter model TT (Innovatis AG, Reutlingen, Germany), which is an electric field multi-channel cell counting system. 50 µl of the cell-suspension were transferred to a CASY-cup and 10 ml of CASYton solution were added. A suitable programme for each cell-line had to be chosen on the Casy model TT prior to starting the measurements. After the measurements, the following values were written down: Total cell-number, number of viable cells and the percentage of the viable cells. Using these values, it was possible to calculate the correct dilution of the primarily prepared cell-suspension and new culture medium, so that a cell number of 0.5×10^6 could be achieved.

2.7.3 Seeding of the cells

For performing cellular experiments, 1×10^6 cells were seeded per 12-well plates (Greiner Bio-One GmbH, Rainbach, Austria) using translucent ThinCert™-cell culture PET inserts with a pore size of 0.4 µm translucent (Greiner Bio-One

GmbH, Rainbach, Austria). 500 µl of the 1 x 10^6 cell concentration solution were transmitted to each cell-culture insert while gently swirling the 12-well plate. As a final step 1500 µl of the culture medium were transferred into the basolateral department. Figure 13 illustrates the compartments schematically.

The cells were incubated overnight and the next day the culture medium was removed from the apical compartment to create air-liquid interface (ALI) culture conditions. ALI culture means that the apical surface of the cells is exposed to air, whereas the basal surface of the cells is in contact with the culture medium of the basolateral compartment. This configuration mimics the conditions of the respiratory airways and inhalation therapy, because drugs are deposited as aerosols onto the air-facing bronchial and alveolar lung epithelium (59). The volume of the medium in the basolateral compartment was reduced to 500 µl to avoid excessive hydrostatic pressure on the cells.

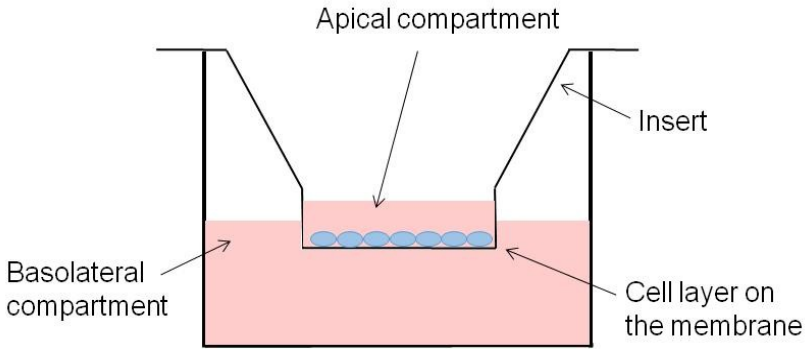

Figure 13: Schematic overview of the insert and its different compartments

2.7.4 Transepithelial electrical resistance (TEER)

TEER measurements were performed every second day to determine the tightness of the cell monolayer. Increasing TEER values imply that the intercellular connections are tightening. As soon as a specific TEER value was reached, the permeability experiments and cellular uptake experiments were started. Because DMBM-2 cells do not form tight junctions, no TEER measurements were performed for this cell line and the cellular experiments were performed one day after seeding the cells.

For the TEER measurements, an EVOM STX-2- electrode and a Milicell® ERS Voltohmmeter (Both from World Precision Instruments, Berlin, Germany) were

used. The electrode has two arms of different length. It is important to make sure, that the shorter arm is put into the apical compartment and the longer arm reaches into the basolateral compartment.
Before starting the measurements, the old culture medium of the basolateral compartment was removed with a pipette and new culture medium was added: 500 µl into the apical compartment and 1500 µl into the basolateral compartment. The electrode then shortly was put into distilled water and directly afterwards the TEER measurements were started by measuring the blank resistance.

The blank resistance represents the resistance of the membrane without a cell layer and is important for calculating the TEER values of the other inserts. The resistances of the other inserts were determined systematically and the value of each insert was taken down. The process of the TEER measurement is illustrated in Figure 14.

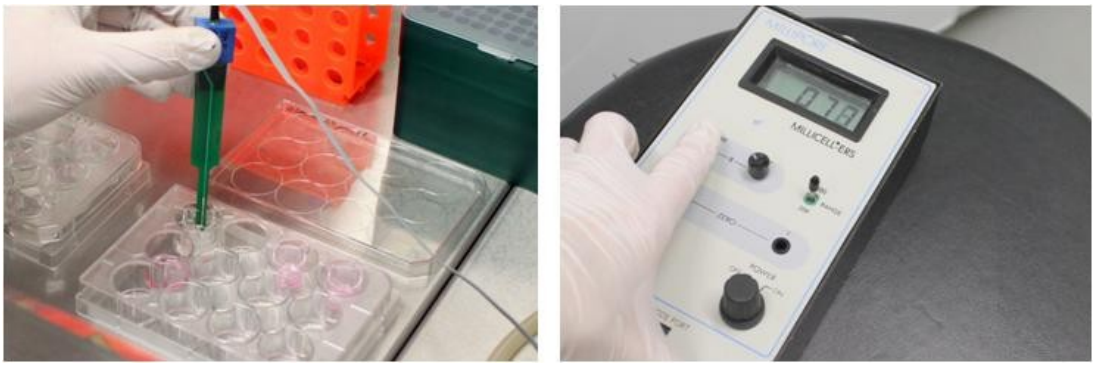

Figure 14: Performing TEER measurements

Afterwards, the TEER values were calculated using the following formula, considering that the membrane area for 12-well inserts is 1.12 cm^2 per well:

*TEER (Ω * cm^2) = (Sample – blank resistance in Ω) * membrane area (cm^2)*

After finishing the TEER measurements, the culture medium was removed from the apical compartment and 500 µl of new culture medium were added to the basolateral compartment.

2.7.5 Cellular experiments

Cellular experiments were performed to determine the permeability and the cellular uptake of salbutamol sulphate with different particle characteristics. Therefore, three different samples of salbutamol sulphate (raw material, jet-milled

and spray dried samples) were applied to the cells on the insert membrane. To determine which concentration of salbutamol sulphate has to be used to receive detectable concentrations for HPLC measurement, a pilot experiment was performed. For this first experiment, raw salbutamol sulphate was used in 4 different concentrations: 50, 100, 200, and 1000 µg/ml. The pre-experiment showed that a concentration of 800 µg/ml has to be used for the following experiments.

In general, the permeability tests were performed with Calu-3 and A549 cells and cellular uptake was determined using A549 and DMBM-2 cells. This decision was made due to the characteristics of the different cell lines. DMBM-2 cells were not used for permeability experiments, because the cells do not form adhesive layers or tight junctions. However, because these cells are macrophages, they are perfectly suitable for determining the cellular uptake of salbutamol sulphate and to check whether the particle shape has an impact on the cellular uptake.

As mentioned above, a salbutamol sulphate concentration of 800 µg/ml was used for all experiments. The three different samples of salbutamol sulphate were suspended in SLF. The experiments were performed under light protected conditions, using a microplate incubator (THERMOstar, BMG LAB TECH GmbH, Ortenberg, Germany) with a temperature of 37°C and a shaking intensity of 200 rpm. Before starting the experiments, the TEER-values were measured not only with culture medium, but also with Krebs-Ringer-Buffer (KRB). The buffer was prepared directly before starting the experiments and contained the following substances: 142 mM NaCL, 3 mM KCl, 1.2 mM $MgCl_2$, 1.5 mM $K_2H_4PO_4$, 4.2 mM $CaCl_2$, 25 mM $NaHCO_3$, 4 mM glucose, 10 mM Hepes (60). The pH was adjusted to 7.4 and afterwards the solution was sterile filtered.

The KRB then was removed from all inserts, except two, and the 12-well plates were placed on the microplate incubator. 510 µl of each formulation (raw, jet-milled and spray dried) were deposited into the apical compartment of the inserts. Each formulation was tested in triplicate, more precisely each formulation was used for three different inserts, guaranteeing reproducible results. Furthermore, one single insert was filled with 510 µl of 0.02 % DPPC and the last two inserts were kept empty, being used for the determination of the cell-number of the inserts.

Figure 15 demonstrates the disposition of the different formulations schematically.

A1 raw SS	**A2** raw SS	**A3** raw SS	**A4** spray-dried SS
B1 spray-dried SS	**B2** spray-dried SS	**B3** jet milled SS	**B4** jet milled SS
C1 jet milled SS	**C2** 0.02% DPPC	**C3** Empty	**C4** Empty

Figure 15: Schematic overview of the formulation disposition

Directly after adding 510 µl of the different formulations into the apical compartment, 10 µl samples were taken from each compartment, representing the initial concentration of salbutamol sulphate at the beginning of the experiment.
To determine the permeability of the different formulations, 1500 µl of KRB were added to each basolateral compartment and immediately afterwards, samples of 100 µl were taken from each compartment (time point: 0 minutes). After 30, 60, 90 and 120 minutes 100 µl samples from the lower departments were taken. Every time a sample was taken, 100 µl of KRB were added to the basolateral compartment to substitute the loss of volume. After 120 minutes a second sample of 10 µl was taken from the apical compartment, representing the end-concentration of salbutamol sulphate in the apical compartment. All samples were directly transferred into vials for HPLC measurements (Figure 16).

The inserts were washed with approximately 0.5 ml of PBS and afterwards 100 ml of Trypsin-EDTA solution were added. The plate was put into the incubator for 2-3 minutes and the trypsin reaction was stopped with 500 µl of culture medium. Subsequently, cells were counted.

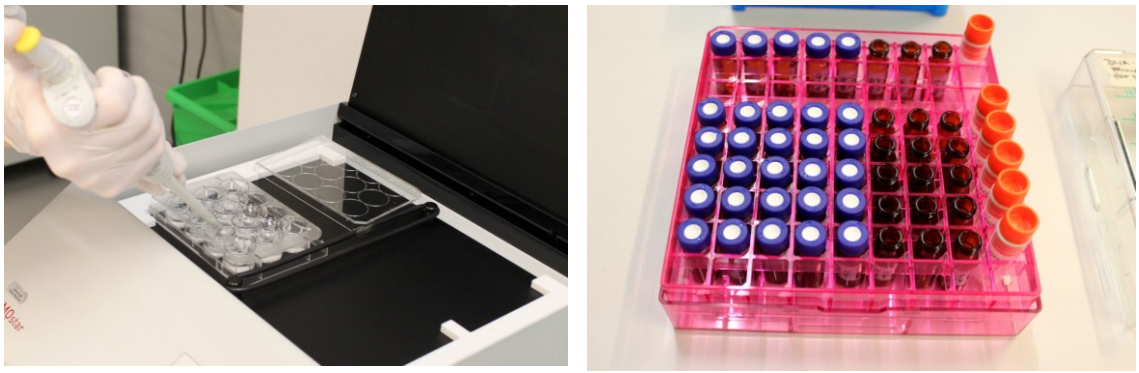

Figure 16: Performing cellular experiments

After all the samples for the permeability experiment had been collected, the remaining volume in the apical and basolateral compartments was removed and transferred into separated and labelled Eppendorf Tubes®, which then were stored in a fridge.

The TEER was measured once more, using KRB and the standard procedure, as described in chapter 2.7.4. This step was performed to check, if the cell-connections had remained intact or had been damaged during the experiment.

As a final step, the cellular uptake was determined. Therefore, 500 µl of a specific solvent (60% of 5mM hexanesulfonic acid sodium salt in water + 1% acetic acid and 40% of methanol) were added to the apical compartment of each insert and the cells were loosened from the insert membrane by carefully scratching the tip of the pipette along the membrane surface. The cells then were resuspended, transferred into specific cyrovials and put into liquid nitrogen for 30 minutes to break up the cell membranes and release salbutamol. Afterwards, the cells were thawed for 30 minutes before being centrifuged for 10 minutes at 4000 rpm. After centrifugation, 333 µl were transferred into HPLC vials and the residue was stored in sterile Eppendorf Tubes® at 20°C.

Prior to the measurements, the samples were diluted with HPLC mobile phase to achieve a proper sample volume for HPLC measurements. The samples from the lower compartment were diluted 1:10, the samples from the apical compartment 1:100 and the cell-suspension samples 1:3.

2.8 HPLC

The salbutamol sulphate concentration of all samples was measured via HPLC (Waters 2695; Waters Corporation, Milford, USA), using an autosampler and a photodiode array detector (Waters 2996), based on a validated HPLC method previously established (48). For all measurements, the following mobile phase was used: 60% of 5mM hexanesulfonic acid sodium salt in water + 1% acetic acid and 40% of methanol. As stationary phase a Luna® 3µm C18 100 Å, LC column was used. Furthermore, a flowrate of 1 ml/min and a column temperature of 30°C were chosen. For each analysis a sample volume of 50 µl was injected into the HPLC system.

2.9 Calculation of P_{app}-values

To compare the permeability of the different formulations, the P_{app} value was calculated. The P_{app} value is the in-vitro apparent permeability coefficient and it is based on the time dependency of the substance transport across the monolayer. It is defined as the following (60):

$$P_{app} = \frac{dQ}{dt \times A \times c}$$

3 Results and discussion

3.1 Particle characterisation

3.1.1 Particle size

Table 4 shows the particle size distribution (PSD) of raw salbutamol sulphate, jet-milled salbutamol sulphate and spray dried salbutamol sulphate, measured via laser diffraction.

Sample	x_{10}/µm	x_{50}/µm	x_{90}/µm
Raw SS	1.13	7.2	20.65
Jet-milled SS	0.65 ± 0.03	2.65 ± 0.08	6.35 ± 0.19
Spray dried SS	0.63 ± 0.02	3.47 ± 0.52	7.4 ± 0.71

Table 4: Particle size distribution of raw SS, jet-milled SS and spray dried SS

X_{90} is a measured diameter, where 90% of the particles contained in the total sample have a smaller particle size than this diameter. X_{10} is defined equally, only that it is the diameter, where 10% of the particles have a smaller particle diameter. In general, these two diameters are always measured by default but a three point specification, including also $X_{50,}$ is considered to be more precisely. X_{50} is the median particle dimension, meaning that 50% of the remaining particles of the total sample are smaller and 50% of the remaining particles are larger than this value (61).

Table 4 shows that both spray dried and jet-milled particles show X_{50} values below 5 µm, whereas raw salbutamol sulphate exhibits X_{50} values higher than 5 µm. Due to this fact, only modified salbutamol sulphate particles can reach the last sections of the human lung and therefore are suitable for inhalation therapy.
However, when comparing the jet-milled and the spray dried particles, it can be seen that the PSD is slightly higher for the spray dried sample than for jet-milled salbutamol sulphate. This leads to the assumption that the modified APIs may also interact differently with the pulmonary cells.

3.1.2 Surface properties

The surface properties and the shape of the different salbutamol sulphate particles (raw, jet-milled and spray dried) were observed using a SEM.

It is already well known that jet-milling mostly leads to needle shaped particles and spray drying to spherical shaped particles. This fact could be confirmed by comparing and analysing the different SEM pictures, shown below (Figure 17-Figure 19).

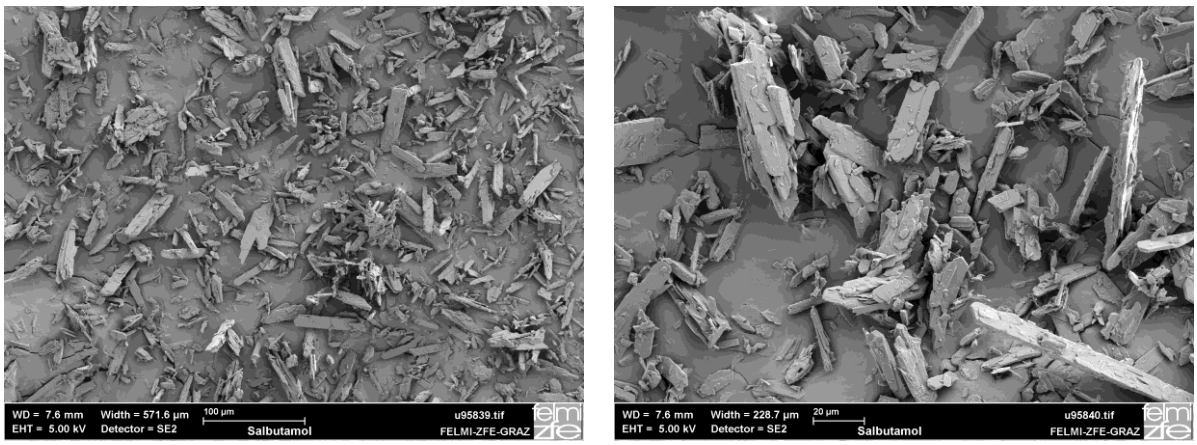

Figure 17: SEM images of raw salbutamol sulphate

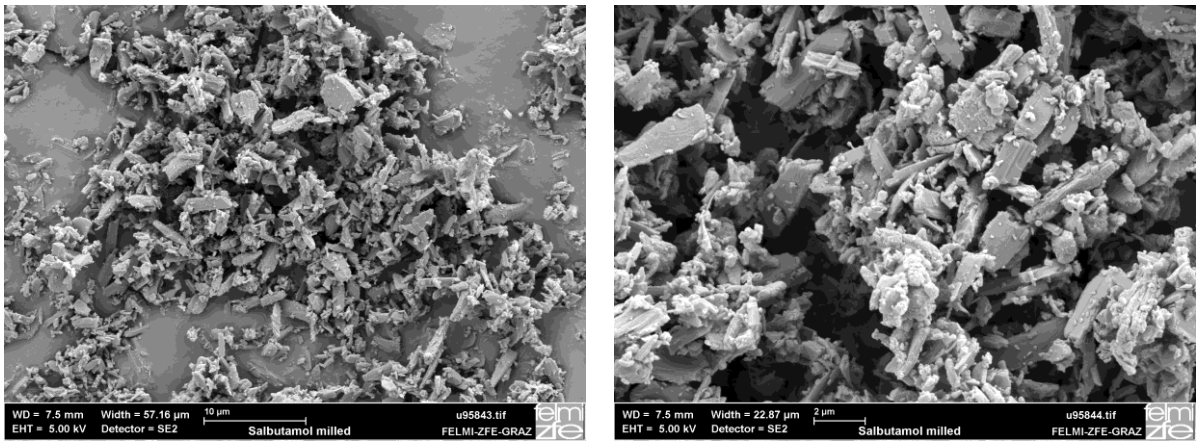

Figure 18: SEM images of jet-milled salbutamol sulphate

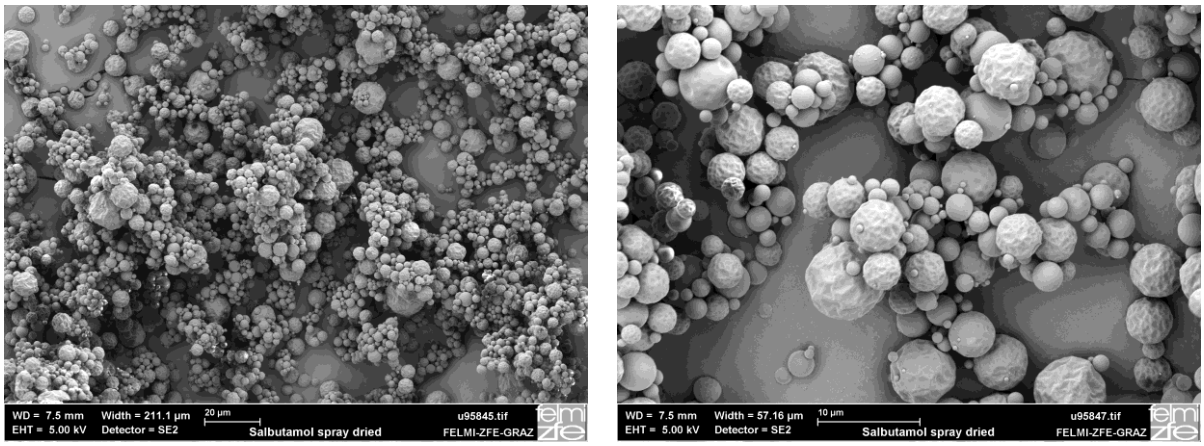

Figure 19: SEM images of spray dried salbutamol sulphate

Figure 17 and Figure 18 show that raw salbutamol sulphate and the jet-milled particles both show needle-like structures. However, the jet-milled particles are smaller than the starting material and it seems that their edges are not as sharp as the edges of raw salbutamol sulphate. Contrarily, spray dried particles are spherical and have partly smooth and partly undulated surfaces, shown in Figure 19.

3.1.3 SWAXS

In order to identify the solid-state of the different particles, SWAXS measurements were performed as described in chapter 2.4.2. It was reported before that jet-milled particles show crystalline structures and spray dried particles show amorphous structures. This could be supported by results from the present study.

When comparing the different graphs, it can be seen that the graph for jet-milled salbutamol sulphate (Figure 20) shows characteristic bragg peaks for crystalline material, described before by Pinto et al (62). On the other hand, amorphous powders lack long-range order in their structure and therefore their graphs do not show any peaks but an amorphous halo.

Comparing the patterns of the jet-milled and the spray dried sample, an obvious difference can be seen, confirming that the samples obtained via spray drying and jet-milling show different solid-state.

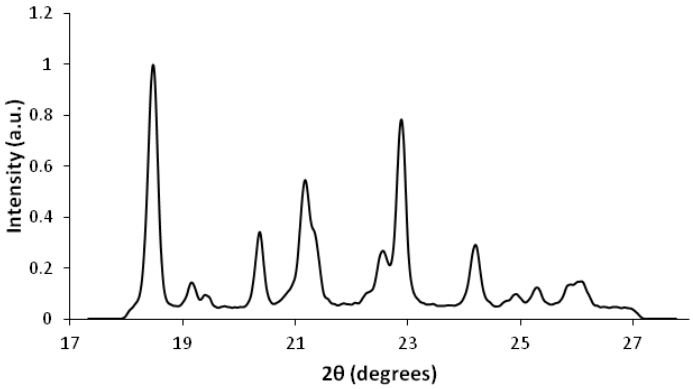

Figure 20: SWAXS pattern of jet-milled salbutamol sulphate

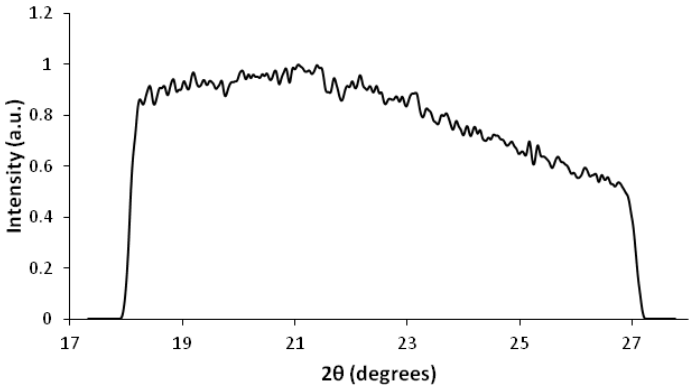

Figure 21: SWAXS pattern of spray dried salbutamol sulphate

3.1.4 DSC

DSC measurements were performed for both jet-milled and spray dried salbutamol sulphate. As already mentioned, during these measurements the glass transition temperature can be determined. After the measurements, characteristic diagrams for both materials were received. The total heat flow of the sample (bottom line) is the sum of the heat capacity component or reversing heat flow (upper line) and the kinetic component or non-reversing heat flow (middle line).

Figure 22 illustrates the graph for jet-milled salbutamol sulphate. The graph shows a characteristic melting of salbutamol sulphate at 184°C with a typical melting enthalpy (ΔH) of approximately 175.5 J/g.

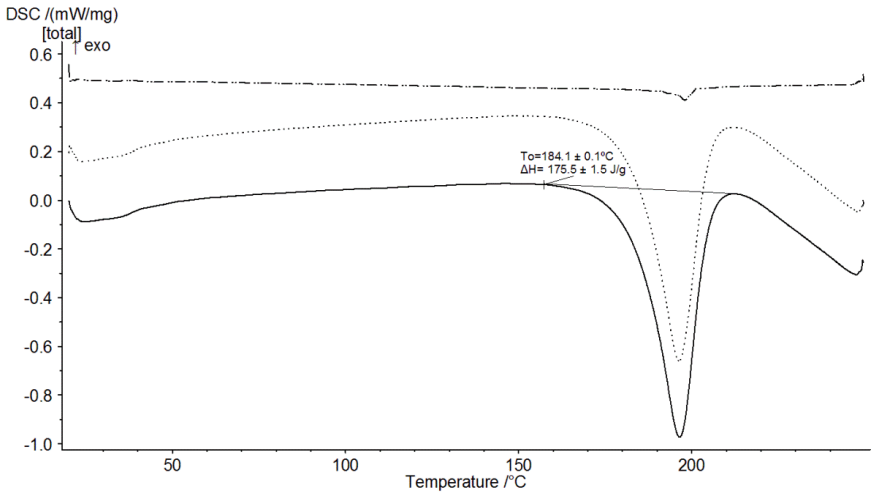

Figure 22: DSC graph for jet-milled salbutamol sulphate

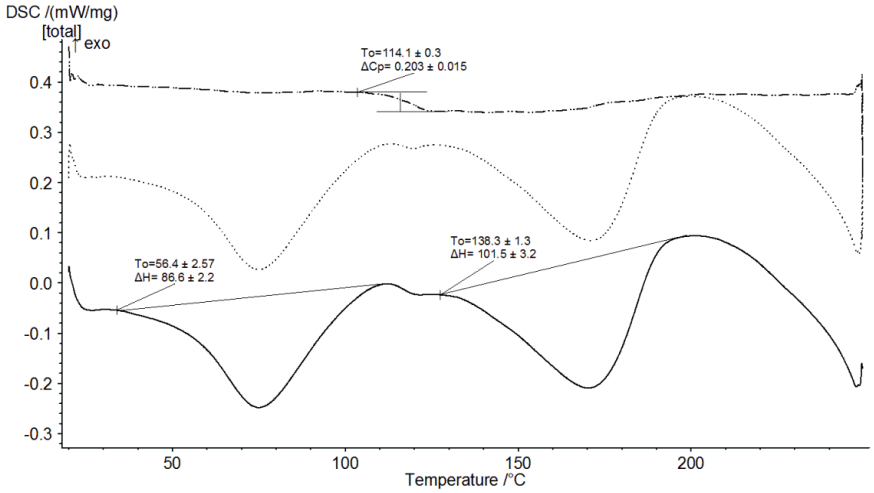

Figure 23: DSC graph for spray dried salbutamol sulphate

The DSC graph of spray dried salbutamol sulphate, illustrated in Figure 23, shows three different peaks, distinguishing it clearly from the jet-milled DSC graph. The first peak most probably represents the evaporation of water, whereas the second peak represents the melting of spray dried salbutamol sulphate at an approximate temperature of 138°C. The measured melting enthalpy was 101.5 ± 3.2 J/g. The sample also showed a glass transition event at 114.1 ± 0.3°C, indicating the amorphous nature of the analysed particles. Although a recrystallization event was expected to be seen at 120°C, it could not be observed. This might be explained by the lower melting temperature of spray dried salbutamol sulphate – the graph of the melting event hides the recrystallization event.

Comparing the DSC diagrams of the modified APIs, it can be seen that spray dried salbutamol sulphate has a lower melting temperature and a lower enthalpy than jet-milled salbutamol sulphate. Furthermore, glass transition could only be observed in spray dried salbutamol sulphate because of its amorphous structure.

3.2 Characterisation of the mixtures

Two different adhesive mixtures with a lactose model carrier were prepared (described in chapter 2.3) in order to perform NGI experiments and dissolution testing of the spray dried and the jet-milled API. To evaluate the quality of the mixtures, SEM images were taken and the mixing homogeneity was determined.

3.2.1 SEM images

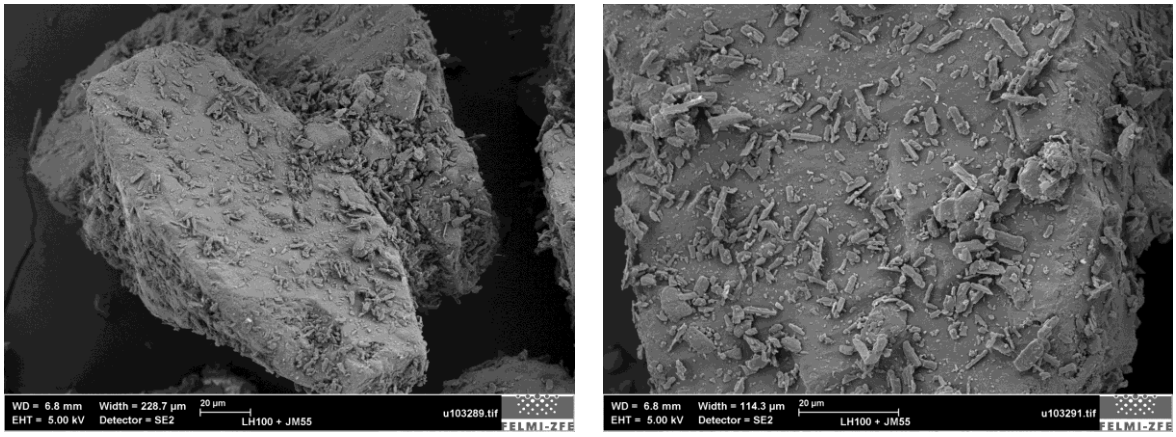

Figure 24: SEM images of LH100 + jet-milled SS

SEM images of Lactohale100 and jet-milled salbutamol sulphate (LH100 + JM SS) show that the needle shaped particles are distributed over the whole carrier surface (Figure 24). By contrast, Figure 25 shows that the spray dried particles are distributed more inhomogeneously over the carrier surface and fewer API-particles are attached to the carrier surface.

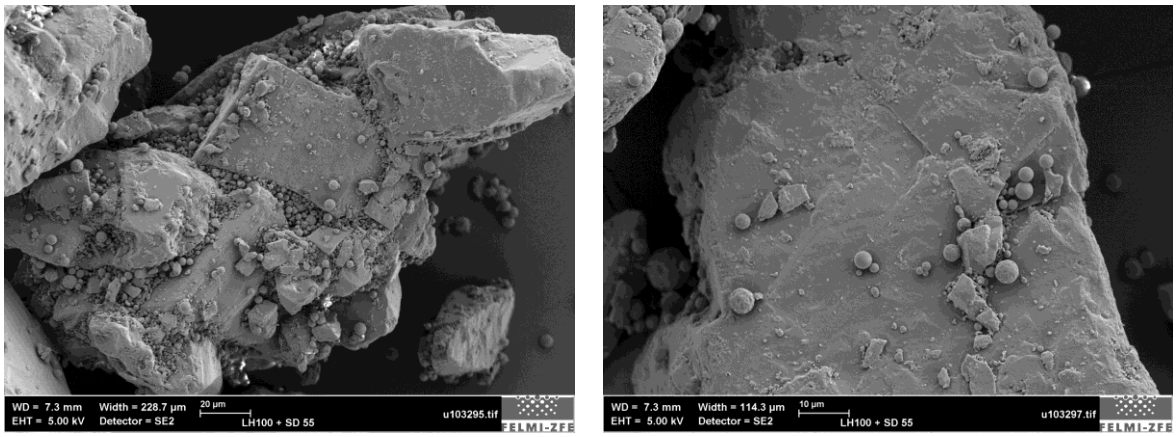

Figure 25: SEM images of LH100 + spray dried SS

3.2.2 Mixing homogeneity and mean drug content

Table 5 shows that the mean drug content recovered is around 2% and therefore matches the target drug content.

Sample	Mean drug content / %	Mixing homogeneity (RSD) / %
LH100 + JM SS	1.99	2.22
LH100 + SD SS	1.89	7.49

Table 5: Mixing homogeneity of the different blends (n=10)

The mixing homogeneity is expressed as the relative standard deviation (RSD) of the mean drug content. In general, it can be said that, the lower the homogeneity values, the higher is the achieved mixture homogeneity. As shown in Table 5, better results were achieved when jet-milled salbutamol sulphate was used for the mixtures, in comparison to spray dried salbutamol sulphate. This is indicated by lower variations of the drug content, respectively the RSD. This data also matches the interpretation of the SEM images, illustrated in chapter 3.2.1. It seems that the jet-milled, needle shaped particles are distributed more homogenously over the carrier surface than the spherical particles of spray dried salbutamol sulphate, which tend to concentrate especially in voids and clefts of the carrier.

3.3 NGI

The following table shows the results of the most important values obtained from NGI measurements. FPF, MMAD and ED were determined for both LH100 + spray dried and LH100 + jet-milled salbutamol sulphate and the standard deviation (SD) was calculated for all values.

Sample	FPF [%]	SD	MMAD [µm]	SD	ED [%]	SD
LH100 + SD SS	12.49	3.28	4.85	0.51	83.23	6.66
LH100 + JM SS	27.68	5.12	2.78	0.23	78.99	9.17

Table 6: NGI results

Results in Table 6 and Figure 26 show, that the FPF of jet-milled salbutamol sulphate is significantly higher than the FPF of spray dried salbutamol sulphate. This is in accordance with previous studies comparing jet-milled and spray dried salbutamol sulphate (63).

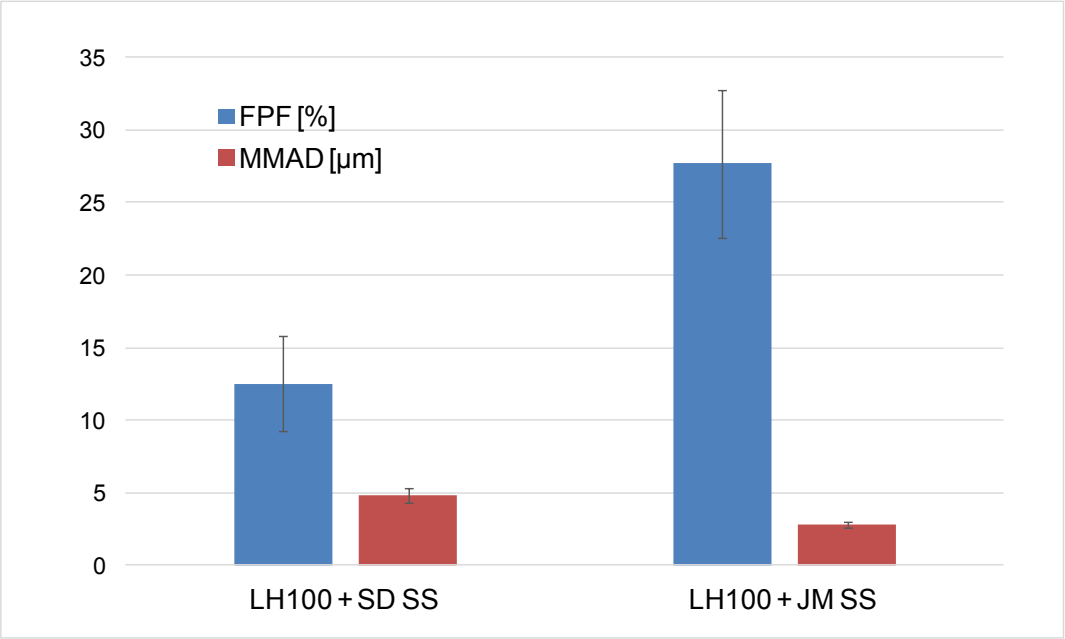

Figure 26: FPF and MMAD for the different mixtures

The ED is around 80% and within the same range for jet-milled and spray dried API. Considering the different FPFs and the same EDs, this indicates that drug detachment from the carrier is more inefficient for spray dried API-particles

compared to the milled API, as the same amount leaves the inhaler but much less API reaches the lung.

The MMAD for jet-milled salbutamol sulphate is lower compared to the MMAD of spray dried salbutamol sulphate. The larger MMAD for the latter indicates particle aggregation. These aggregates could possibly not be fully dispersed during inhalation what in turn could also explain the low FPF compared to the same ED of the two formulations.

3.4 Dissolution

The results of the dissolution experiments (Figure 27 - Figure 29) showed no significant difference between the two formulations. Both jet-milled and spray dried salbutamol sulphate rapidly dissolve in SLF and it can be seen that after 2 minutes nearly the total amount of the API is dissolved. Therefore it can be assumed that the shape of the particles has very little impact on the solubility of a good soluble drug. Additionally, the impact of the particle shape on biological effects in the lung may also be very little, since the drug substance dissolves rapidly and loses its particle shape.

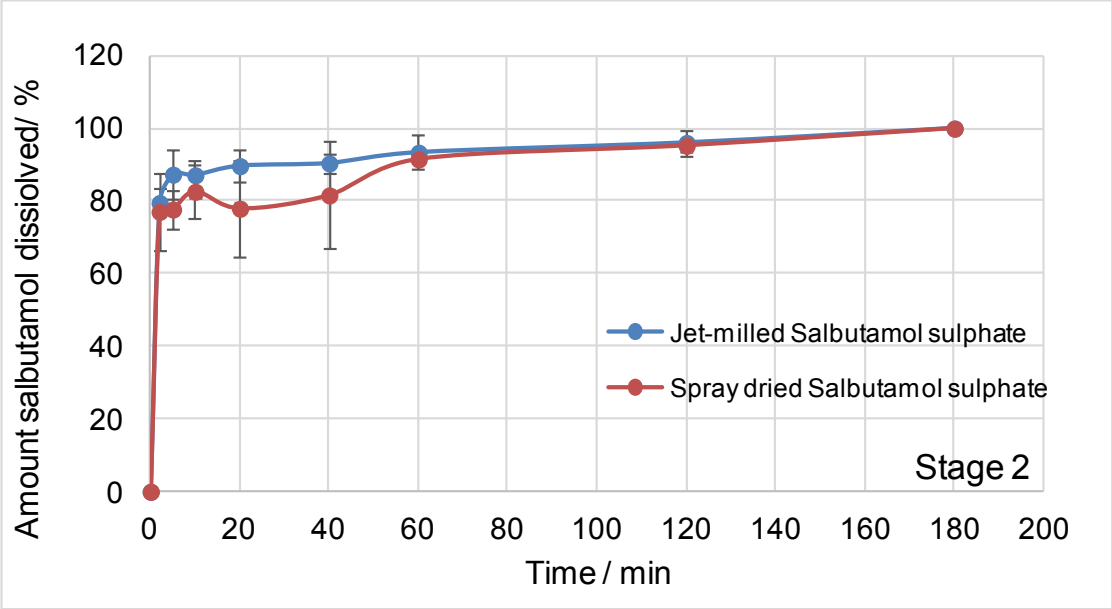

Figure 27: Results of dissolution experiments for stage 2

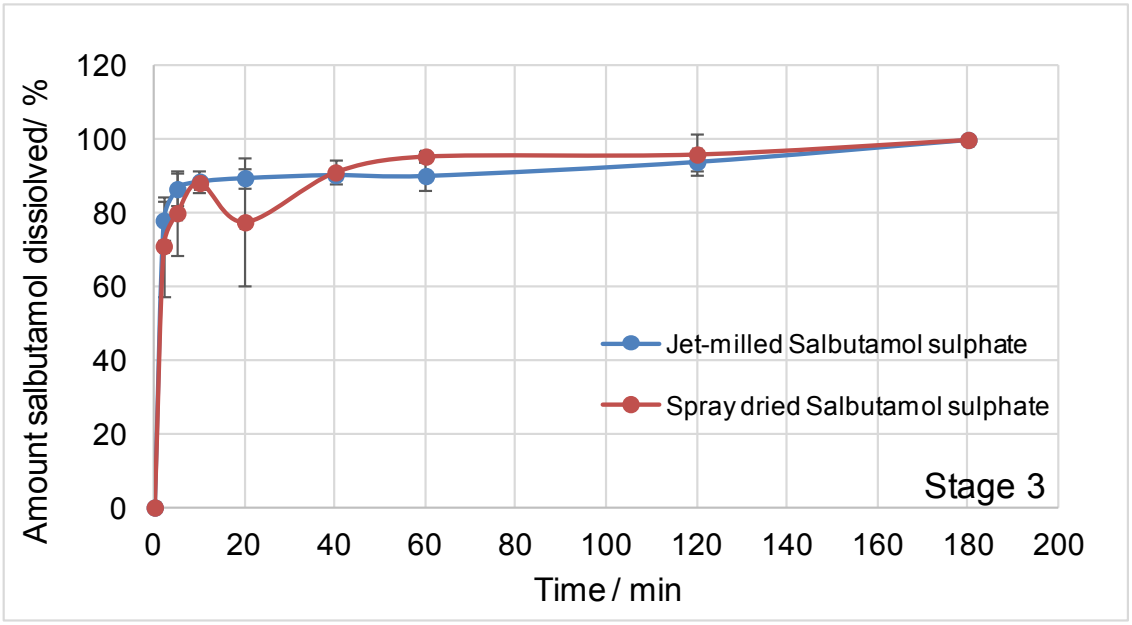

Figure 28: Results of dissolution experiments for stage 3

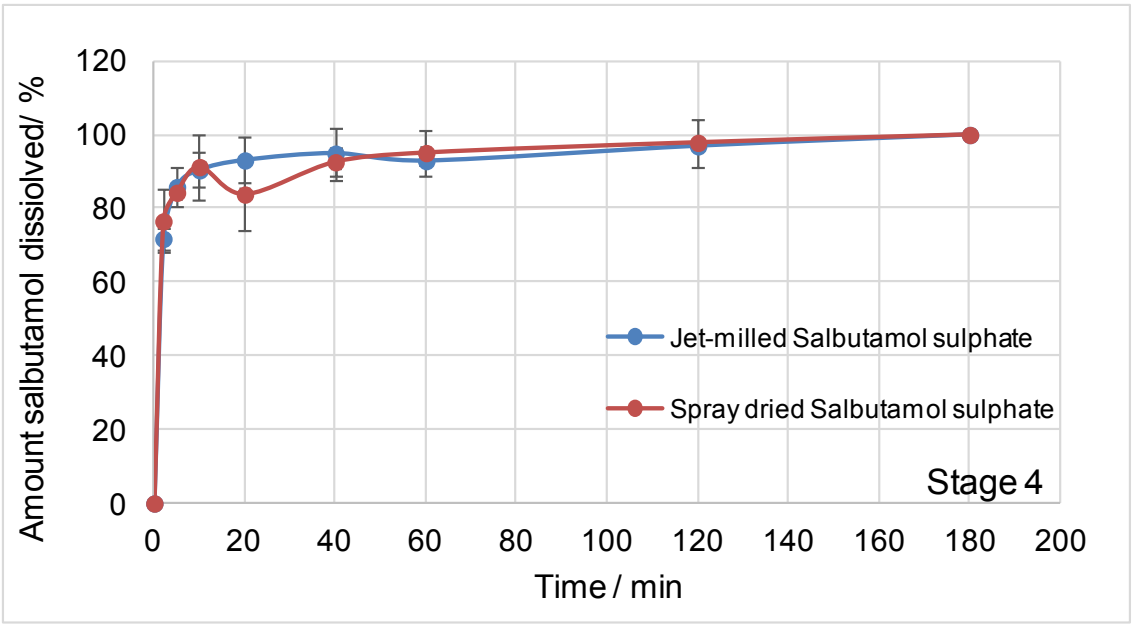

Figure 29: Results of dissolution experiments for stage 4

It can be seen that the spray dried formulation dissolves slightly slower than the jet-milled formulation and shows higher variations. This fact may have an influence on the results of the permeability experiments, which also show more instable results for spray dried salbutamol sulphate. Again, the formation of particle aggregates of the spray dried material and the resulting delayed dissolution of the

aggregates (representing larger particle sizes) could explain the variations in the dissolution.

3.5 Cell studies

As already mentioned, two main biological functions were determined via cellular experiments, namely permeability and cellular uptake. These biological functions are essential for pulmonary drug delivery. The aim of the experiments was to identify whether the different formulations of salbutamol sulphate lead to differences regarding the cellular uptake and the permeability. Furthermore, for each experimental set up, two different cell lines were used. Therefore, it was possible to identify also differences between the differing cell lines regarding their cellular uptake and the permeability of salbutamol sulphate.

3.5.1 Permeability

Calu-3 cells and A549 cells were used for permeability experiments. Both cell lines represent in-vitro systems for pulmonary epithelial cells. Calu-3 cells are used as a model for bronchial epithelial cells, whereas A549 cells represent type II alveolar epithelial cells. The cell lines differ, however, in the tightness of their intercellular junctions. This difference can be seen in Figure 30, which illustrates the TEER-values of A549 and Calu-3 cells after 8 days in medium.

Inserts	TEER-values (Ω/cm²) A549 cells	TEER-values (Ω/cm²) Calu-3 cells
A1	11	935
A2	24	886
A3	15	869
A4	19	860
B1	17	914
B2	32	1057
B3	27	1018
B4	23	928
C1	20	935
C2	15	954
C3	25	998
C4	19	944

Figure 30: TEER-values of A549 and Calu-3 cells, measured on day 8 in medium

The diagrams on the following page graphically illustrate the permeability of the different salbutamol sulphate formulations over time. As described in section 2.7.5, samples were taken after 0, 30, 60, 90 and 120 minutes from the basolateral compartment and the corresponding salbutamol sulphate concentration at each time point was determined via HPLC. In general, an increasing salbutamol sulphate concentration could be observed because the particles pass the cellular layers on the membranes and penetrate into the basolateral department.

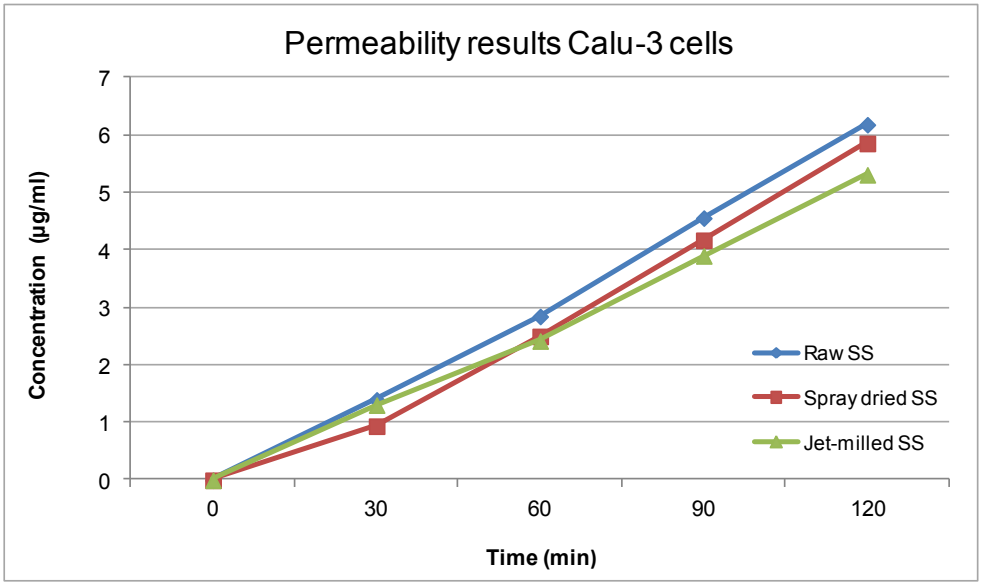

Figure 31: Permeability results of Calu-3 cells

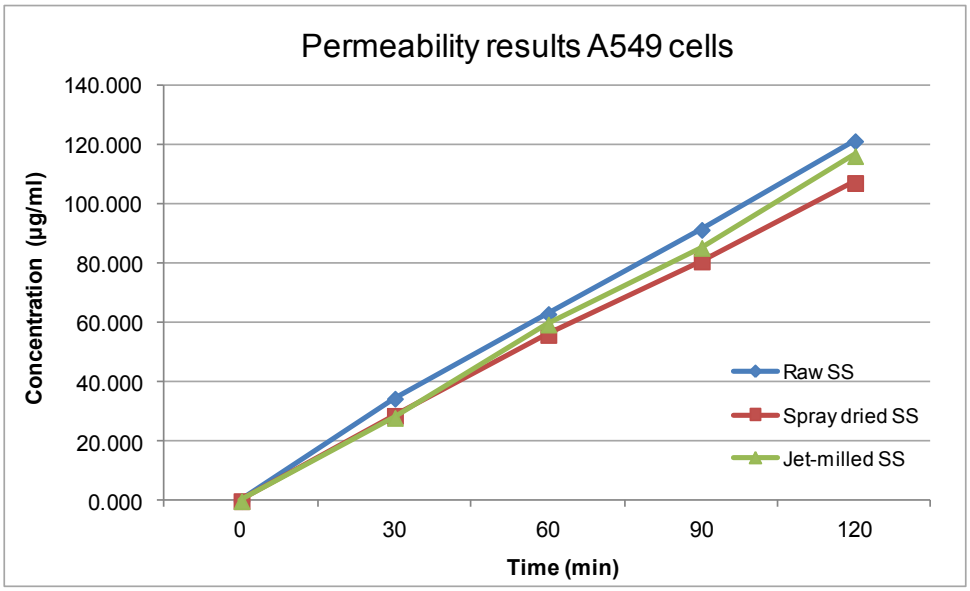

Figure 32: Permeability results of A549 cells

Comparing the two cell-types, it can be seen that the transport of raw salbutamol sulphate was significantly higher when using A549 cells. In the same manner, the concentration of jet-milled and spray dried salbutamol sulphate was also higher in A549 cells. Salbutamol sulphate is a hydrophilic molecule, which is mainly transported between cells (paracellular transport). Since A549 cells possess less tight junctions, salbutamol can pass the monolayer to much higher extend than Calu-3 monolayers with higher TEER-values.

The transport of salbutamol sulphate in all formulations was linear, suggesting that no active transporters are involved. If receptor-mediated transport is involved, time-dependent transport follows a saturation curve (64).Taking standard deviation (data not shown) into account and as seen in the graphs, no difference between the different formulas for each cell type could be observed.

Table 7 and Table 8 show the P_{app} values for the different formulations and the two different cell lines.

A549 cells		
Sample	**P_{app} (cm/s)**	**SD (n=3)**
Raw SS	1.5085 E-05	1.0759 E-06
Jet-milled SS	1.5938 E-05	4.0039 E-07
Spray dried SS	1.6163 E-05	2.9564 E-07

Table 7: P_{app} values for A549 cells

Calu-3 cells		
Sample	**P_{app} (cm/s)**	**SD (n=3)**
Raw SS	8.3401 E-07	4.8934 E-08
Jet-milled SS	8.5348 E-07	1.1003 E-07
Spray dried SS	1.4036 E-06	7.6044 E-07

Table 8: P_{app} values for Calu-3 cells

As it can be seen in the table, the P_{app} values for all three formulations are similar, but a slightly higher value could be achieved when spray dried salbutamol sulphate was used. The standard deviation was highest for jet-milled salbutamol sulphate.

When Calu-3 cells were used, the P_{app} values in general were lower, compared to the values for A549 cells (E-07, E-06 compared to E-05). P_{app} values in this study are in the same order of magnitude compared to the values reported by Bur et al. (2.8 ± 1.6 E-07 cm/s) (65) and lower than the P_{app} values reported by Ehrhardt et al. (1.9 ± 0.25 E-06 cm/s) (66). A direct comparison of the values from the literature is not possible, because they were obtained from Calu-3 cells, which

were not cultured in ALI-condition. The effect of the tightness of the intercellular junctions in clearly visible; P_{app} values of salbutamol sulphate across A549 cells were about 10 times higher than P_{app} values of Calu-3 cells.

3.5.2 Cellular uptake

Data show higher uptake of SS in DMBM-2 cells, mainly referable to their cell-type (Table 9 and Table 10). As already mentioned, DMBM-2 cells are murine macrophages, which phagocytise particles similarly to human macrophages. The main function of macrophages is the uptake of foreign material, pathogens and damaged cells via phagocytosis.

DMBM-2 cells		
Sample	Cellular uptake (µg/Mio cells)	SD (n=3)
Raw SS	3.5069	0.5097
Jet-milled SS	2.1838	0.5211
Spray dried SS	4.0822	1.5102

Table 9: Cellular uptake, DMBM-2 cells

A549 cells		
Sample	Cellular uptake (µg/Mio cells)	SD (n=3)
Raw SS	1.5891	0.2237
Jet-milled SS	1.3766	0.1739
Spray dried SS	1.4840	0.2048

Table 10: Cellular uptake, A549 cells

In general, there are two different endocytotic uptake mechanisms: pinocytosis and phagocytosis. Whereas pinocytosis, which includes macropinocytosis, caveolin-mediated endocytosis, clathrin-mediated endocytosis and clathrin- and caveolin independent endocytosis, involves the uptake of fluids and particles within small vessels, phagocytosis mainly applies to the uptake of larger particles (67). Furthermore, phagocytosis is carried out only by professional phagocytes, namely monocytes, macrophages, dendritic cells and neutrophilic granulocytes. The cellular uptake is influenced by several different parameters but size, shape and surface properties are the most decisive particle-related parameters and might influence the relation of phagocyte to non-phagocyte uptake. More precisely, phagocytosis affects only particles, which have a diameter greater than 0.5 µm. Particles with diameters smaller than 0.5 µm are too small to trigger phagocytosis. Pinocytosis, on the contrary, occurs in all cells and macropinocytosis covers a broad range of particle sizes ranging from 100 nm to 5 µm (68).

As seen in Table 4, the mean particle size of the spray dried and jet-milled salbutamol sulphate particles is approximately 3 µm. Due to their size, the

particles could perfectly be taken up by the macrophages via phagocytosis. However, as discussed in section 3.4, the particles dissolve rapidly in SLF because salbutamol sulphate is a very soluble drug. It can be assumed, that during the dissolution process, the particle size diminishes. Therefore it is rather unlikely, that the particles are taken up via phagocytosis, which means that other uptake mechanisms, such as macropinocytosis, must occur. It has been reported that macrophages possess also higher uptake rates by other routes. The pinocytosis rate of murine fibroblasts 18.7 μm^3/h/cell compared to 46.5 μm^3/h/cell in murine peritoneal macrophages (69,70)

4 Conclusion and outlook

In this study spherical, predominantly amorphous and needle shape, crystalline particles of salbutamol sulphate were generated via two different engineering techniques in order to investigate the impact of particle shape on biological effects in the lung.

This study confirmed results previously described for salbutamol sulphate particles. Particle engineering of SS and the resulting distinct particle properties, like particle shape, impacts the *in-vitro* aerosolization behaviour. The inhalation performance (higher fine particle fraction) is significantly improved for jet-milled SS compared to spray dried SS. Spray dried, spherical and predominantly amorphous particles resulted in lower FPFs, compared to the jet-milled, needle shaped and predominantly crystalline particles, when blended and tested with a lactose model carrier. This could probably be explained by the agglomeration tendency of spray dried amorphous salbutamol sulphate particles and the insufficient drug dispersion and detachment during inhalation.

By contrast, spray dried particles showed higher P_{app} values and higher uptake by macrophages compared to the jet-milled particles. The fact that rod-shaped but not needle-shaped particles are better targets than spherical particles for macrophages and the larger size of the spherical particles could well explain the preferential uptake of these particles by macrophages. The extremely fast dissolution, on the other hand, argues against a prominent role of particle shape and size because it was reported that only 20-40% of 2 µm particles had been ingested by macrophages after 2 minutes of incubation (71).

Dissolution tests of formulations containing spray died and jet-milled drug particles revealed quite fast dissolution of both APIs, independent of their shape, due to the good solubility of SS in water. Nevertheless, dissolution profile of spray dried particles showed larger variations. This could probably also be related to particle agglomerates of different sizes that show modified and retarded dissolution depending on the size of agglomerates. In future experiments, an API with lower solubility will be tested in order to evaluate the influence of shape on cellular uptake in more detail. Moreover, to better attribute changes either to shape or other properties like solid-state, additional needle shaped-amorphous particles will be generated e.g. via milling.

List of references

1. Schmitz F. Brust-, Bauch- und Beckensitus: Teil G: 2 Atmungsorgane und Pleura. In: Aumüller G, Aust G, Engele J, editors. Duale Reihe Anatomie [Internet]. 3rd ed. Stuttgart: Georg Thieme Verlag; 2014. p. 541–76. Available from: http://www.thieme-connect.de/products/ebooks/abstract/10.1055/b-0034-100799

2. Weibel ER, Sapoval B, Filoche M. Design of peripheral airways for efficient gas exchange. Respir Physiol Neurobiol. 2005;148(1–2 SPEC. ISS.):3–21.

3. Florens M, Sapoval B, Filoche M. An anatomical and functional model of the human tracheobronchial tree. J Appl Physiol [Internet]. 2011;110(3):756–63. Available from: http://jap.physiology.org/content/110/3/756.long

4. McNulty W, Usmani OS. Techniques of assessing small airways dysfunction. Eur Clin Respir J [Internet]. 2014;1:25898–http://dx.doi.org/10.3402/ecrj.v1.25898. Available from: http://www.ncbi.nlm.nih.gov/pmc/articles/PMC4629724/

5. Lüllmann-Rauch R. Atmungsorgane. In: Taschenlehrbuch Histologie. 5th ed. Stuttgart; New York: Georg Thieme Verlag; 2012. p. 348–65.

6. Anderhuber F, Filler TJ, Pera F, Peuker ET. Innere Organe in Thorax , Abdomen und Becken. In: Anderhuber F, Pera F, Streicher J, editors. Waldeyer - Anatomie des Menschen. 19th ed. Berlin; Boston: De Gruyter; 2012. p. 427–601.

7. Klar F, Urbanetz NA. Darreichungsformen, Formulierungen und Depositionscharakteristika: Arzneiformen der Betasympathomimetika. Pharm Unserer Zeit. 2011;40(5):390–402.

8. Fronius M, Clauss WG, Althaus M. Why do we have to move fluid to be able to breathe? Front Physiol. 2012;3 MAY(May):1–9.

9. Hartmann M, Pabst M-A, Dohr G, Schmied R. Respirationstrakt. In: Zytologie, Histologie und mikroskopische Anatomie. 5th ed. Wien: facultas.wuv; 2011. p. 77–81.

10. Akella A, Deshpande SB. Pulmonary surfactants and their role in pathophysiology of lung disorders. Indian J Exp Biol. 2013;51(1):5–22.

11. Silbernagl S, Despopoulos A. Atmung. In: Taschenatlas Physiologie [Internet]. 8th ed. Stuttgart; New York: Thieme; 2012. p. 112–45. Available from: https://www-1thieme-2connect-1de-19783135677088.han.medunigraz.at/products/ebooks/book/10.1055/b-002-50992

12. Herold G. Pneumologie. In: Innere Medizin. Köln: Herold; 2016. p. 332–434.

13. Quint JK, Millett ERC, Joshi M, Navaratnam V, Sara L, Hurst JR, et al. Europe PMC Funders Group Changes in the incidence , prevalence and mortality of bronchiectasis in the UK from 2004-2013 : a population based cohort study. 2016;47(1):186–93.

14. Farrell PM. The prevalence of cystic fibrosis in the European Union.

2008;7:450–3.

15. Castellani C, Assael BM. Cystic fibrosis : a clinical view. Cell Mol Life Sci. 2017;74(1):129–40.

16. Asthma and COPD prevalence. Heal a Glance Eur State Heal EU Cycle. 2016;82–4.

17. Böcker W, Denk H, Heitz PU, Moch H, Höfler G, Kreipe H. Erkrankungen der Bronchien. In: Böcker W, editor. Pathologie [Internet]. 5th ed. München; Jena: Elsevier, Urban und Fischer; 2012. p. 482–6. Available from: https://institut-1elsevierelibrary-1de-1978-23-2437-242384-20.han.medunigraz.at/pdfreader/pathologie

18. To T, Stanojevic S, Moores G, Gershon AS, Bateman ED, Cruz AA, et al. Global asthma prevalence in adults : findings from the cross-sectional world health survey. BMC Public Health [Internet]. 2012;12(1):204. Available from: http://www.biomedcentral.com/1471-2458/12/204

19. Arastèh K. Krankheiten der unteren Atemwege. In: Arastèh K, editor. Duale Reihe Innere Medizin. 3rd ed. Stuttgart: Thieme; 2013. p. 369–85.

20. Fehrenbach H, Wagner C, Wegmann M. Airway remodeling in asthma: what really matters. Cell Tissue Res [Internet]. 2017;551–69. Available from: http://ovidsp.ovid.com/ovidweb.cgi?T=JS&PAGE=reference&D=medp&NEWS=N&AN=28190087

21. Lewis MJ, Short AL, Lewis KE. Autonomic nervous system control of the cardiovascular and respiratory systems in asthma. Respir Med. 2006;100(10):1688–705.

22. Rubin BK, Priftis KN, Schmidt HJ, Henke MO. Secretory hyperresponsiveness and pulmonary mucus hypersecretion. Chest [Internet]. 2014;146(2):496–507. Available from: http://dx.doi.org/10.1378/chest.13-2609

23. Papiris S, Kotanidou A, Malagari K, Roussos C. Clinical review: severe asthma. Crit Care [Internet]. 2002;6(1):30–44. Available from: http://www.ncbi.nlm.nih.gov/pubmed/11940264%5Cnhttp://www.pubmedcentral.nih.gov/articlerender.fcgi?artid=PMC137395

24. Pierce R. Spirometry: An essential clinical measurement. Aust Fam Physician. 2005;34(7):535–9.

25. Sim YS, Ph D, Lee J, Ph D, Lee W, Ph D, et al. Spirometry and Bronchodilator Test. 2017;3536:105–12.

26. PEF and MEF | Spirohub [Internet]. spirohub. 2015 [cited 2017 May 16]. Available from: http://spirohub.com/2015/06/13/sh03/

27. Pulmonary Function Tests [Internet]. [cited 2017 Jun 20]. Available from: http://www.sharinginhealth.ca/respiratory/investigations/pulmonary_function_tests.html

28. Jia CE, Zhang HP, Lv Y, Liang R, Jiang YQ, Powell H, et al. The asthma control test and asthma control questionnaire for assessing asthma control:

Systematic review and meta-analysis. J Allergy Clin Immunol [Internet]. 2013;131(3):695–703. Available from: http://dx.doi.org/10.1016/j.jaci.2012.08.023

29. Asthma bronchiale [Internet]. amboss.miamed.de. 2017 [cited 2017 May 11]. Available from: https://amboss.miamed.de/library#xid=Ph0WVf&anker=54cba6aac118008b633463d369dead7e

30. Bergmann K-C. Asthma bronchiale – viele Formen, viele Therapien. DMW - Dtsch Medizinische Wochenschrift [Internet]. 2016;141(10):687–92. Available from: http://www.thieme-connect.de/DOI/DOI?10.1055/s-0042-104795

31. Hassett DJ, Borchers MT, Panos RJ. Chronic obstructive pulmonary disease (COPD): Evaluation from clinical, immunological and bacterial pathogenesis perspectives. J Microbiol. 2014;52(3):211–26.

32. Vestbo J, Hurd SS, Agustì AG, Jones PW, Vogelmeier C, Anzueto A, et al. Global strategy for the diagnosis, management, and prevention of chronic obstructive pulmonary disease GOLD executive summary. Am J Respir Crit Care Med. 2013;187(4):347–65.

33. Bagdonas E, Raudoniute J, Bruzauskaite I, Aldonyte R. Novel aspects of pathogenesis and regeneration mechanisms in COPD. Int J Chron Obstruct Pulmon Dis [Internet]. 2015;10:995–1013. Available from: http://www.dovepress.com/novel-aspects-of-pathogenesis-and-regeneration-mechanisms-in-copd-peer-reviewed-article-COPD

34. Ukena D, Sybrecht GW. Erkrankungen der Atemwege. In: Alexander K, editor. Thiemes Innere Medizin. Stuttgart [u.a.]: Thieme; 1999. p. 1473–516.

35. New 2017 GOLD Guidelines for COPD Released - PulmCCM [Internet]. [cited 2017 Jun 20]. Available from: http://pulmccm.org/main/2016/copd-review/new-2017-gold-guidelines-copd-released/

36. Clini E, Costi S, Lodi S, Rossi G. Non-pharmacological treatment for chronic obstructive pulmonary disease. Med Sci Monit [Internet]. 2003;9(12):RA300-5. Available from: http://www.ncbi.nlm.nih.gov/pubmed/14646985

37. Nielsen M, Bårnes CB, Ulrik CS. Clinical characteristics of the asthma – COPD overlap syndrome – a systematic review. 2015;1443–54.

38. Sin DD. Asthma-COPD Overlap Syndrome: What We Know and What We Don't. Tuberc Respir Dis (Seoul) [Internet]. 2017;80(1):11. Available from: https://synapse.koreamed.org/DOIx.php?id=10.4046/trd.2017.80.1.11

39. Katzung BG, Masters SB, Trevor AJ. Basic & clinical pharmacology. In: 12th ed. McGraw-Hill Lange; 2012.

40. Unwalla HJ, Horvath G, Roth FD, Conner GE, Salathe M. Albuterol modulates its own transepithelial flux via changes in paracellular permeability. Am J Respir Cell Mol Biol. 2012;46(4):551–8.

41. Beubler E. Atemwege. In: Kompendium der Pharmakologie. 3rd ed. Wien: Springer; 2011. p. 85–93.

42. Cazzola M, Page CP, Calzetta L, Matera MG. Pharmacology and Therapeutics of Bronchodilators. Pharmacol Rev [Internet]. 2012;64(3):450–504. Available from: http://pharmrev.aspetjournals.org/cgi/doi/10.1124/pr.111.004580%5Cnpapers2://publication/doi/10.1124/pr.111.004580%5Cnfile:///C:%5CUsers%5Cmbirrhl%5CDropbox%5CMendeley Desktop/Cazzola et al. - 2012 - Pharmacology and Therapeutics of Bronchodilators.pdf

43. Lüllmann H, Mohr K, Wehling M, Hein L. Respirationstrakt. In: Pharmakologie und Toxikologie. 18th ed. Stuttgart; New York: Georg Thieme Verlag; 2016. p. 213–22.

44. Qiu Y, Lam J, Leung S, Liang W. Delivery of RNAi Therapeutics to the Airways—From Bench to Bedside. Molecules [Internet]. 2016;21(10):1249. Available from: http://www.mdpi.com/1420-3049/21/9/1249

45. Dolovich MB, Ahrens RC. Device Selection and Outcomes of Aerosol Therapy : Evidence-Based Guidelines * American College of Chest Physicians / American College of Asthma , Allergy , and Immunology. Chest [Internet]. 2005;127(1):335–71. Available from: http://dx.doi.org/10.1378/chest.127.1.335

46. Labiris NR, Dolovich MB. Pulmonary drug delivery. Part II: The role of inhalant delivery devices and drug formulations in therapeutic effectiveness of aerosolized medications. Br J Clin Pharmacol. 2003;56(6):600–12.

47. Pepper AN, Cooke A, Livingston L, Lockey RF. Asthma and chronic obstructive pulmonary disease inhalers: Techniques for proper use. Allergy asthma proc. 2016;37(4):279–90.

48. Faulhammer E, Wahl V, Zellnitz S, Khinast JG, Paudel A. Carrier-based dry powder inhalation: Impact of carrier modification on capsule filling processability and in vitro aerodynamic performance. Int J Pharm. 2015;491(1–2):231–42.

49. ADMIT - online info [Internet]. [cited 2017 Oct 7]. Available from: http://www.admit-online.info/index.php?id=342&L=0

50. Salbutamol sulfate | C13H23NO7S - PubChem [Internet]. [cited 2017 Jun 12]. Available from: https://pubchem.ncbi.nlm.nih.gov/compound/9884233#section=Top

51. Inhalation Grade Lactose for dry powder inhalers [Internet]. [cited 2017 Jun 12]. Available from: http://www.dfepharma.com/en/excipients/inhalation-lactose/lactohale-100.aspx

52. Mitchell JP, Nagel MW, Nichols S, Nerbrink O. Laser diffractometry as a technique for the rapid assessment of aerosol particle size from inhalers. J Aerosol Med. 2006;19(4):409–33.

53. Liu L, Boldon L, Urquhart M, Wang X. Small and Wide Angle X-Ray Scattering Studies of Biological Macromolecules in Solution. J Vis Exp [Internet]. 2013;(71):2–7. Available from: http://www.jove.com/video/4160/small-wide-angle-x-ray-scattering-studies-biological-macromolecules

54. Xiang K, Xiaoping C. Review of Dry Powder Inhaler Devices | American Pharmaceutical Review - The Review of American Pharmaceutical Business & Technology [Internet]. 2016 [cited 2017 Dec 3]. Available from: http://www.americanpharmaceuticalreview.com/Featured-Articles/185892-Review-of-Dry-Powder-Inhaler-Devices/

55. How to use aerolizer? Istanbul allergy center [Internet]. [cited 2017 Dec 3]. Available from: http://www.istanbulallergy.com/how-to-use-aerolizer/

56. Rohrschneider M, Bhagwat S, Krampe R, Michler V, Breitkreutz J, Hochhaus G. Evaluation of the Transwell System for Characterization of Dissolution Behavior of Inhalation Drugs: Effects of Membrane and Surfactant. Mol Pharm [Internet]. 2015 Aug 3 [cited 2017 Jun 20];12(8):2618–24. Available from: http://pubs.acs.org/doi/abs/10.1021/acs.molpharmaceut.5b00221

57. Foster KA, Avery ML, Yazdanian M, Audus KL. Characterization of the Calu-3 cell line as a tool to screen pulmonary drug delivery. Int J Pharm. 2000;208(1–2):1–11.

58. Foster KA, Oster CG, Mayer MM, Avery ML, Audus KL. Characterization of the A549 Cell Line as a Type II Pulmonary Epithelial Cell Model for Drug Metabolism. Exp Cell Res [Internet]. 1998 Sep [cited 2017 Jun 20];243(2):359–66. Available from: http://linkinghub.elsevier.com/retrieve/pii/S0014482798941726

59. Stemcell Technologies Inc. Air-Liquid Interface Culture For Respiratory Research. 2016 [cited 2017 Dec 6]; Available from: https://cdn.stemcell.com/media/files/techbulletin/TB29885-Air_Liquid_Interface_Culture_Respiratory_Research.pdf?_ga=2.99578334.139802930.1512587248-792603643.1512587248

60. Meindl C, Stranzinger S, Dzidic N, Salar-Behzadi S, Mohr S, Zimmer A, et al. Permeation of therapeutic drugs in different formulations across the airway epithelium in vitro. PLoS One. 2015;10(8):1–19.

61. Zaidi K, Moore K. Harmonization Stage 6: 429 Light Diffraction Measurement of Particle Size. Pharmacopeial forum [Internet]. 2016;35(3):707. Available from: https://www.usp.org/sites/default/files/usp/document/harmonization/gen-chapter/g13_pf_35_3_2009.pdf

62. Pinto JT, Radivojev S, Zellnitz S, Roblegg E, Paudel A. How does secondary processing affect the physicochemical properties of inhalable salbutamol sulphate particles? A temporal investigation. Int J Pharm [Internet]. 2017;528(1–2):416–28. Available from: http://dx.doi.org/10.1016/j.ijpharm.2017.06.027

63. Zellnitz S, Faulhammer E, Wutscher T, Khinast J, Paudel A. Drug Delivery to the Lungs. In: Impact of particle engineering on the processability and aerosolization performance of DPI formulations. 2016.

64. Brewer E, Lowman AM. Assessing the transport of receptor-mediated drug-delivery devices across cellular monolayers. J Biomater Sci Polym Ed.

2014;25(5):455–73.

65. Bur M, Huwer H, Muys L, Lehr C-M. Drug Transport Across Pulmonary Epithelial Cell Monolayers: Effects of Particle Size, Apical Liquid Volume, and Deposition Technique. http://www.liebertpub.com/jamp [Internet]. 2010 [cited 2017 Oct 8]; Available from: http://online.liebertpub.com/doi/abs/10.1089/jamp.2009.0757?url_ver=Z39.88-2003&rfr_id=ori%3Arid%3Acrossref.org&rfr_dat=cr_pub%3Dpubmed&

66. Ehrhardt C, Kneuer C, Bier C, Lehr C-M, Kim K-C, Bakowsky U. Salbutamol is actively absorbed across human bronchial epithelial cell layers. Pulm Pharmacol Ther [Internet]. 2005 [cited 2017 Oct 8];18(3):165–70. Available from: http://www.sciencedirect.com/science/article/pii/S1094553904001567?via%3Dihub

67. Kuhn DA, Vanhecke D, Michen B, Blank F, Gehr P, Petri-fink A, et al. Different endocytotic uptake mechanisms for nanoparticles in epithelial cells and macrophages. 2014;1625–36.

68. Hirota K, Terada H. Endocytosis of Particle Formulations by Macrophages and Its Application to Clinical Treatment. In: Molecular Regulation of Endocytosis [Internet]. INTECH; 2012. Available from: http://www.intechopen.com/books/molecular-regulation-of-endocytosis

69. Edelson PJ, Zwiebel R, Cohn ZA. The pinocytic rate of activated macrophages. J Exp Med. 1975;142:1150–63.

70. Steinman RM, Silver JM, Cohn ZA. Pinocytosis in fibroblasts: Quantitative studies in vitro. J Cell Biol. 1974;63(3):949–69.

71. Paul D, Achouri S, Yoon Y, Herre J, Bryant CE, Cicuta P. Phagocytosis Dynamics Depends on Target Shape. Biophys J. 2013;105(5):1143–50.